A modelling-based assessment of suspended sediment transport related to new damming in the Red River basin from 2000 to 2013

Xi Wei, Sabine Sauvage, Sylvain Ouillon, Thi Phuong Quynh Le, Didier Orange, Marine Herrmann, Jose-Miguel Sanchez-Perez

A modelling-based assessment of suspended sediment transport related to new damming in the Red River basin from 2000-2013

Xi Wei[1*], Sabine Sauvage[1**], Sylvain Ouillon[2,3], Thi Phuong Quynh Le[4], Didier Orange[5], Marine Herrmann[2,3], José-Miguel Sanchez-Perez[1]

[1]ECOLAB, Université de Toulouse, CNRS, INPT, UPS, Auzeville-Tolosane, France.

[2]LEGOS, Université de Toulouse, IRD, CNRS, UPS, Toulouse, France.

[3]USTH, Vietnam Academy of Science and Technology (VAST), Hanoi, Vietnam.

[4]Institute of Natural Product Chemistry (INPC), Vietnam Academy of Science and Technology (VAST), Hanoi, Vietnam.

[5]Eco & Sols, Univ. Montpellier, IRD, CIRAD, INRA, Montpellier SupAgro, Montpellier, France.

Correspondence

*Xi Wei, ECOLAB, Université de Toulouse, CNRS, INPT, UPS, Avenue de l'Agrobiopole, 31326 Auzeville-Tolosane, France.

Email: xi.wei_fr@hotmail.com

**Sabine Sauvage, ECOLAB, Université de Toulouse, CNRS, INPT, UPS, Avenue de l'Agrobiopole, 31326 Auzeville-Tolosane, France.

Email: sabine.sauvage@univ-tlse3.fr

Abstract:

The Red River is an Asian river system strongly affected by global changes. This paper aims to characterize and quantify the suspended sediment flux (SF) over the basin under the influences of short-term climate variability and dam constructions. SF was evaluated at the outlets of main tributaries and along the main course of the Red River from 2000 to 2013 based on daily simulations from a modelling study. A reference scenario (without dams) was carried out to disentangle the impacts of short-term climate variability and damming by comparing to actual conditions. Without dams (reference scenario), the basin would generate 106.9 Mt yr^{-1} of SF to the downstream delta from 2000 to 2013, with a specific sediment yield (SSY) of 778.8 t km^{-2} yr^{-1}. However, under the impacts of short-term climate variability and dams, the mean annual SSY decreased to 84.5 t km^{-2} yr^{-1}. At the outlet of the basin, the annual mean SF of 2008-2013 (after new dam constructions) got reduced by 90% (10% related to short-term climate or atmospheric variability and 80% to dam constructions) compared to the reference scenario (without dams) during 2000-2007. The Thao tributary is the most sensitive to short-term climate variability while the Da tributary is mostly affected by the huge-capacity dams. Mean annual retentions of sediment by dams ranged from 7.1 to 111.0 Mt yr^{-1}. Simple rating curves between monthly mean discharge (Q) and SF were established for estimating SF at the outlet of the tributaries and the Red River. High soil erosion (above 2000 t km^{-2} yr^{-1}) occurred in the middle Thao and the lower Da

tributaries. Precipitation, slope and agriculture practices are the key influence factors for soil erosion in the basin.

Keywords: suspended sediment, modelling, the Red River, short-term climate variability, dam, soil erosion.

1. INTRODUCTION

The suspended sediment (SS) transport from continents to oceans by rivers is a crucial process of sediment cycle in the Earth systems: this process drives associated elements to the seas, which is essential for marine biogeochemical cycle and diversity; also, it is a reflection of land and river degradation; besides, this process is of great importance in geomorphology, such as downstream delta formation (Dai et al., 2009; Kunz et al., 2011; Lal et al., 1995). Rivers contribute to 95% of the sediment fluxes (SF) to the oceans (Syvitski et al., 2003), which ranged from 15 to 20 billion t yr^{-1} (Beusen et al., 2015; Ludwig and Probst, 1996; Milliman and Meade, 1983; Ouillon, 2018; Vörösmarty et al., 2003). In particular, Asian rivers such as the Yellow River and the Mekong River contribute to a large part of sediment delivery to the seas (Cohen et al., 2014; Dang et al., 2018). However, climate variability and anthropogenic activities have altered the SF (Dai et al., 2009; Dang et al., 2018; Jiang et al., 2009).

Under anthropogenic disturbances such as intensive agriculture and damming, water ecosystems are facing severe challenges, like the increase of soil erosion, and changes of hydrology regime and SF (Chen et al., 2016; FAO, 2011a; IPCC, 2019; Valentin et al., 2008; Zimmerman et al., 2008). Dam

67 construction is the factor with the strongest influence on land-ocean SF
68 (Walling and Fang, 2003). According to the World Commission on Dams
69 (2000), at least 45,000 large dams have been built globally, and nearly half of
70 the world's rivers have one large dam at least. Lehner et al., (2011) found that
71 around 28% of dams are located in Asia. Besides, future hydropower
72 development is primarily concentrated in developing countries and emerging
73 economies of Southeast Asia (Zarfl et al., 2015). Dams cause a significant
74 reduction in SF. Vörösmarty et al. (2003) estimated that the potential sediment
75 trapping by dams in regulated basins was higher than 50%. In some basins,
76 such as the Colorado, Nile and Yellow rivers, sediment is completely trapped
77 due to the large size of reservoirs and to the flow velocity decreases which
78 weakens the sediment transportability (Peng et al., 2010; Vörösmarty et al.,
79 2003; Walling and Fang, 2003). Reduced sediment transport can induce river
80 deltas sinking, therefore affecting estuarine and coastal human communities
81 (Hauer et al., 2018; Syvitski et al., 2005), and increasing their vulnerability
82 (Lehner et al., 2011). Asian rivers constitute good indicators of the strong
83 influence of anthropogenic activities on sediment transport (Arias et al., 2014;
84 Dang et al., 2010; Furuichi et al., 2009).

85 The Red River is a typical Asian river system under the influences of global
86 changes and is the second largest river in Vietnam. It gathers numerous
87 inter-linked rivers, estuaries and coastal waters and plays an important role in
88 agriculture and economy in this basin, which is a major agricultural production
89 region. Understanding and quantifying the water and soil processes and

budgets of this river basin will help to manage soil loads and also to study other Asian rivers. Hence, the objective of this paper is to assess the SS regime in a large Asian basin under the influences of global changes, especially under the impacts of dams. Moreover, it would be more precise to calculate SF at a daily time step as discharge (Q) and suspended sediment concentration (SSC) can vary greatly from day to day. However, few studies analyzed fluxes at daily scale in the Red River basin, focusing either on a short period (Le et al., 2007), or only on the outlet of the continental basin (Dang et al., 2010) or on the delta (Luu et al., 2010), or only on Q or SS (Hiep et al., 2018). Assessing SS regime at a daily time step at different stations in the Red River basin will, therefore, contribute to improving our knowledge of the SF across the whole basin.

For achieving this objective, a modelling approach, combining remote sensing and in-situ data, was used. The modelling setup and calibration were described in Wei et al. (2019). The specific objective of the present paper is: 1) to quantify SF of the Red River basin based on daily Q and SSC; 2) to disentangle and quantify the impacts of damming and short-term climate or atmospheric variability on SF; 3) to provide rating curves for estimating the SF at the outlets of the main tributaries and of the continental basin; 4) to identify the hot spots of soil erosion.

2. MATERIALS AND METHODS

2.1. Study area

The study area focuses on the Red River continental basin with a surface of

137,200 km^2 which drains down to Son Tay, the outlet of the continental basin and the entrance of the delta (Figure 1).

2.1.1. General characteristics

The Red River basin is located in Southeast Asia (Figure 1a), shared by China (49%), while Vietnam (50.1%) and Laos (0.9%).

Son Tay is a confluence of three main tributaries: the Lo River (named Panlong Jiang in China) on the left bank, the Thao River (named Yuan Jiang in China) upstream of the main river, and the Da River (named Lixian Jiang in China) on the right bank. They join the Red River 20 km upstream to the Son Tay gauging station.

The elevation ranges from 2650 m a.s.l. to 6 m a.s.l. in this basin (Wei et al., 2019). The upstream part of Lao Cai is mainly formed by tectonically active mountainous areas, with steep slopes, usually above 25° (Zhang et al., 2017) which are vulnerable to soil erosion due to the intensive precipitation and land use changes (Bai et al., 2015; Barton et al., 2004; He et al., 2007). The soil types are mainly Acrisols, such as red earth and yellow-brown soil (Bai et al., 2015; Le, 2005). High erosion plus the character of soil types color the water of the Thao River into “red” (Le, 2005). In Vietnam, the same Acrisols dominate on the slopes while grey or alluvial soils dominate in the valleys (Le et al., 2017).

In China’s part, the main land cover is forest (62%), followed by grassland (19%) and cultivated land (18%), respectively (Li et al., 2016a). In Vietnam’s

part, in the Thao basin, forest is dominating, accounting for 54.2%, followed by rice paddy fields (19%) and industrial crops (13%); the Lo and Da basins are dominated by industrial crops (58%) and forests (74%), respectively (Le et al., 2007).

Figure 1. (a) The geographical location of the Red River basin in Southeast Asia; (b) locations of the dams (red triangle) and the hydrological gauge stations (blue point) in the Red River basin.Base maps sources were obtained from ArcGIS desktop.

2.1.2. Meteorological characteristics

The whole Red River basin encompasses two different climate zones: humid subtropical climate in the upper part and humid tropical climate in the lower part, and a strong seasonal variability related to the Southeast Asia monsoon system, which alternates between the cold and dry southwestward winter monsoon from November to April and the hot and humid northeastward summer monsoon from May to October. Rainfall during flood seasons (May to October) contributes to 85-90% of the whole year average (Le et al., 2007; Li et al., 2016b). The general trend of regional precipitation distribution increases from upstream (1000 to 1600 mm yr^{-1} in China) to downstream (1328 to 2255 mm yr^{-1} in Vietnam) (Le et al., 2007; Li et al., 2008; Xie, 2002). During 2000-2013, the mean annual rainfall through the Red River basin was 1494 mm yr^{-1} (Wei et al., 2019).

Temperature variations follow a typical orographic pattern, increasing with the decreasing of the elevations, from the northwest (mountainous regions) to the

158 southeast. The mean annual temperature varies from 15 to 21 °C in China (Xie,
159 2002) and 14 to 27 °C in Vietnam (Le, 2005). During the year, the winter
160 temperature ranges from 14-16 °C in winter and 27-29 °C in summer (Le, 2005;
161 Lu et al., 2015).

162 2.1.3. Hydrological characteristics

163 Runoff is mainly recharged by precipitation which leads to big seasonal
164 variations in river flows (FAO, 2011b; Li et al., 2016a; Li et al., 2008). The
165 mean annual discharge during 2000-2013 at Son Tay was 3082 $m^3 s^{-1}$ (Wei et
166 al., 2019). Corresponding to the distribution of rainfall, the runoff is also
167 unevenly distributed. More than 80% of the total annual runoff is produced
168 during rainy seasons (May to October); runoff peaks usually occur in August,
169 and the maximum flood reached 8050 $m^3 s^{-1}$ in 1986 near the border in China
170 (Xie, 2002), and 37,800 $m^3 s^{-1}$ at Son Tay in 1971 (Luu et al., 2010). November
171 to April is the dry season, and the minimum discharge occurs in March. The
172 minimum discharge observed near the boundary in China was 28.7 $m^3 s^{-1}$ in
173 1963 (Ren et al., 2007), and the minimum daily discharge at Son Tay during
174 2000-2013 was 493 $m^3 s^{-1}$ (Wei et al., 2019).

175 2.1.4. Dams implementation

176 In recent years, to meet the water demand according to the rapid increase of
177 population and intensive agriculture activities, dams have been constructed
178 both in China and Vietnam. It is difficult to obtain all the information of all the
179 dams located in the Thao and Lo rivers as most of their information is not
180 accessible to the public, therefore, in this study, we only specifically took into

account the dams with big capacity (>2.2 km^3) and located on the downstream part, i.e. close to the outlets of each tributary.

On the Thao River, twelve cascade reservoirs were built or are under construction in China's territory. The impoundment of the first two dams, the Nansha and the Madushan dams, located around 150 km and 100 km upstream of Lao Cai gauge station respectively, started on November 2007 and December 2010, respectively, and they are the only two dams impounded on the Thao River during the study period.

On the Da River, the biggest dam in Vietnam named Hoa Binh was put into use in 1989. A mass of solid materials has been trapped by this dam, which consequently reduces the dam's efficient capacity and lifetime (Dang et al., 2010). To mitigate the siltation of the Hoa Binh dam and to meet the need for economic growth, the Son La dam was built and put into operation in January 2011.

On the Lo River, the Thac Ba dam was implemented in 1972 and the Tuyen Quang dam in March 2008 (Table 1 and Figure 1).

Table 1 Basic characteristics of the main dams in the Red River basin (Le et al., 2017; Wei et al., 2019)

2.2. Data collection

Observed data of daily Q and SSC from 2000 to 2013 was obtained from the Vietnam Ministry of Natural Resources and Environment (MONRE) at Lao Cai, Yen Bai, Vu Quang, Hoa Binh and Son Tay gauge stations (Figure 1). Daily SS

sampling campaigns were conducted at different gauge stations. SS was collected vertically from the water surface to the bottom by a collector at each station. Then in the laboratory, a known volume of well-mixed sample was filtered immediately by vacuum filtration through precombusted glass fiber filters. For the measurement of SS, each filter was dried for 2 hours at 105°C and then weighed. Taking into account the filtered volume, the increase in weight of the filter represented the total SS per unit volume (mg L^{-1}).

Daily SF, calculated from daily Q and SSC, was used to evaluate the model. Annual mean and seasonal variation of observed Q and SSC for 2000-2013 at these stations are presented in Table 2.

Table 2 Annual mean and seasonal variation of observed discharge (Q) and suspended sediment concentration (SSC) for 2000-2013 at 5 gauge stations.

2.3. Modelling approach

This study expands the work of Wei et al. (2019) where detailed descriptions of the modelling setup and the calibration and validation processes can be found. Here we only present some essential information about the modelling.

In the study of Wei et al. (2019), the daily simulated Q and SSC were presented. In this study, we dug and analyzed the outputs from the model, providing more information within this basin, such as the soil erosion which is an influencing factor for SF; and also we stated how the outputs from the modelling can be beneficial for the stakeholders.

225 2.3.1. The SWAT model

226 The Soil and Water Assessment Tool (SWAT) is a physically-based,
227 semi-distributed hydrological model. It considers soils, land use and
228 management conditions to predict the impact of land management practices
229 on water and sediment within large complex basins where there might be no
230 monitoring data over long periods of time (Neitsch et al., 2009).

231 Both hydrological and sediment dynamics in SWAT are simulated in two
232 components: over the land, and in the channel network. More information
233 about SWAT hydrological can be found in Arnold et al. (1998) and Neitsch et al.
234 (2009).

235 To calculate the sediments from the landscape component, SWAT computes
236 the erosion caused by rainfall with the Modified Universal Soil Loss Equation
237 (MUSLE) for each HRU (Neitsch et al., 2009; Williams, 1975). This equation
238 considers the surface runoff volume, peak runoff rate, soil erodibility, land
239 cover and management, topographic and coarse fragment factor, as follows:

$$sed = 11.8 \cdot \left(Q_{surf} \cdot q_{peak} \cdot area_{hru}\right)^{0.56} \cdot K_{USLE} \cdot C_{USLE} \cdot P_{USLE} \cdot LS_{USLE} \cdot CFRG \quad (1)$$

240 where sed is the sediment yield on a given day (t), $\mathrm{Q_{surf}}$ is the surface runoff
241 volume (mm H_2O ha^{-1}), $\mathrm{q_{peak}}$ is the peak runoff rate (m^3 s^{-1}), $\mathrm{area_{hru}}$ is the area
242 of the HRU (ha), $\mathrm{K_{USLE}}$ is the USLE soil erodibility factor which is related to the
243 properties of the soil itself (0.013 ton m_2 hr/(m^3 ton cm)), $\mathrm{C_{USLE}}$ is the USLE land
244 cover and management factor (defined as the ratio of soil loss from land
245 cropped under specified conditions to the corresponding loss from clean-tilled,

continuous fallow), P_{USLE} is the USLE support (agricultural) practice factor (defined as the ratio of soil loss with a specific support practice, such as contour tillage, strip cropping and terrace systems, to the corresponding loss with up-and-down slope culture), LS_{USLE} is the USLE topographic factor calculated according to the slopes of the basin, and $CFRG$ is the coarse fragment factor.

The sediment routing in the channel is a function of two processes: deposition and degradation, operating simultaneously in the reach. The Simplified Bagnold equation (1977) is used as a default method for the sediment routing in stream channels which determines degradation as a function of channel slope and flow velocity. The maximum amount of sediment that can be transported is a function of the peak channel velocity, as follows:

$$conc_{sed,ch,mx} = c_{sp} \cdot {v_{ch,pk}}^{spexp} = c_{sp} \cdot \left(\frac{q_{ch,pk}}{A_{ch}}\right)^{spexp} = c_{sp} \cdot \left(\frac{prf \cdot q_{ch}}{A_{ch}}\right)^{spexp} \quad (2)$$

where $conc_{sed,ch,mx}$ is the maximum concentration of sediment that can be transported by the water (t m^{-3}), c_{sp} is a coefficient defined by the user, $v_{ch,pk}$ is the peak channel velocity (m s^{-1}), $spexp$ is an exponent defined by the user, $q_{ch,pk}$ is the peak flow rate (m^3 s^{-1}), A_{ch} is the cross-sectional area of flow in the channel (m^2), prf is the peak rate adjustment factor, and q_{ch} is the average rate of flow (m^3 s^{-1}).

2.3.2. SWAT data inputs

The topography, land cover and soil maps of the Red River basin for the model

266 are presented here to give a better understanding of the characteristic of the
267 Red River basin (Figure 2, Wei et al., 2019). The climate inputs including daily
268 temperature and precipitation were obtained from remote sensing databases:
269 Climate Forecast System Reanalysis (CFSR) and Tropical Rainfall Measuring
270 Mission (TRMM, product 3B42 V7). The CFSR is a global, high resolution and
271 reanalysis product, coupled atmosphere-ocean-land surface-sea-ice system
272 designed to provide the best estimate of the state of these coupled domains
273 over this period. CFSR, combining with hydrology models, has been proved to
274 result in similar accuracy for computing Q as using surface observation data on
275 large river basins (Dile and Srinivasan, 2014; Lauri et al., 2014). Simons et al.
276 (2016) compared several satellite-based precipitation products to actual
277 evapotranspiration products in the Red River basin and found that TRMM
278 rainfall product could provide reliable values in both space and time at this
279 basin. The resolutions and downloading sources of the above inputs can be
280 found in the supplementary material (Table S-1).

281

282 Figure 2: (a) digital elevation model (gray shades); (b) slope classes: slopes were divided into 5 classes by
283 SWAT based on the (DEM); (c) land use map; (d) soil types. Data sources are presented in the
284 supplementary material (Table S-1), and the legends of land use and soil are detailed in the
285 supplementary material (Tables S-2 and S-3).

286 2.3.3. Model set up

287 The whole basin was divided into 242 sub-basins by model based on 1) the
288 characteristics of the basin according to the input data (DEM, soil property and
289 land use); 2) the gauge stations and sampling sites; 3) dam locations; 4)

harmonized size of all the sub-basins.

The main large dams in Table 1 were added to the model. In order to disentangle and quantify the impacts of the dams, two scenarios were simulated (Figure 3): (a) actual conditions with the existing dams; (b) reference scenario without dams. The difference between these two scenarios was the dam implementations. New dams mainly started to operate in 2008, therefore, the study period was divided into two sub-periods (pre-new-dams: 2000-2007 and post-new-dams: 2008-2013) to evaluate the total impact from old and new dams.

The hydrological parameters were kept the same for both periods (pre-new-dams and post-new-dams) for both the actual conditions and the reference scenario. Sediment parameters in Equation (1) and (2) were the same for pre-new-dams and post-new-dams periods except for the parameter c_{sp} which expresses the river bed erodibility. The dam implementations change the particle size distribution downstream, leading to a change in the channel erodibility (Wei et al., 2019). Therefore, c_{sp} was decreased from 0.008 for the pre-new-dams period to 0.002 for the post-new-dams period. For the reference scenario, the sediment parameters were kept the same as the pre-new-dams of the actual conditions. The sediment parameters setting is presented in Table S-4 in the supplementary material.

The simulation was carried out and calibrated on a daily scale from 2000 to 2013 and analyzed at different temporal scales (daily, monthly and annual).

Figure 3. Scenarios setting: actual conditions and reference scenario. Gray triangles are the old dams built before 2000 and black triangles are the new dams built after 2007.

2.3.4. Model evaluation and validation

Based on the daily-scale simulation, simulated monthly and annual SF were extracted to compare with observed data for checking the performance of the model. Following the recommendations by Moriasi et al. (2007), coefficient of determination (R^2), Nash–Sutcliffe Efficiency (NSE), and Percent Bias (PBIAS) were used to evaluate the simulations.

Results from the reference scenario were validated by comparing to the results from Lu et al. (2015), Vinh et al. (2014) and Dang et al. (2010).

2.4. Estimating the impacts of short-term climate variability and dams on SF

By comparing the mean annual SF of reference scenario between 2000-2007 and 2008-2013, the impacts of short-term climate variability can be quantified (Figure 3). By comparing the mean annual SF during 2008-2013 between actual conditions and reference scenarios, the impacts of dams can be quantified. By comparing the mean annual SF of actual conditions between 2000-2007 and 2008-2013, the impacts of four new dams and short-term climate variability can be quantified.

In this study, we hypothesized that the impact of the land use changes during our study period was not significant. Some researchers used a modelling approach to examine the impacts of land use changes on SF in Vietnam and found that an 11-16% decrease in forest land was likely to increase 3.0-3.9%

SF (Khoi and Suetsugi, 2014; Phan et al., 2010). In the Red River basin, between 2000 and 2010, the forest percentage stayed the same, and the farmland increased by 8% from bare land (Le et al., 2018), which might cause less than 2% increase of SF according to Khoi & Suetsugi (2014) and Phan et al. (2010). Therefore, we took into account the impact of land uses on SF but not of its changes during the study period.

2.5. Q-SF simple relationships

Another advantage of this modelling approach is that from the outputs of the modelling, the relationships (rating curves) between Q and SF can be inferred at any point within this basin, which enables people to estimate SF at any point with limited Q data. In this study, we would explore and present the relationships between monthly mean Q and SF for the 5 gauge stations as an example to show the benefits of this modelling. The results are presented in section 3.3. Different temporal scale relationships, such as daily or annual Q-SF relationships, can also be inferred by using the outputs of the modelling.

2.6. Identifying the influencing factors of soil erosion from landscape

The SS in the river can come from both hillslope soil erosion and channel processes. Therefore, having an insight into the land soil erosion can help people understand the source of the SS.

Hot spots of land soil erosion were identified according to the model outputs, and the main triggering factors were determined from the correlations between them and SF according to the principal component analysis (PCA) method

358 described below.

359 PCA was used in this study to identify the factors influencing soil erosion in this
360 basin. More detailed explanations of this method can be seen in Basilevsky
361 (1994), Lever et al. (2017), Ringnér (2008) and Wold et al. (1987). Based on
362 the parameters in Equation (1) and (2) and the analysis of parameters in the
363 study of Wei et al. (2019), the following variables of each sub-basin were
364 added into the PCA model to identify the main factor involved in SE in the
365 basing: soil erosion (SE), precipitation (P), water yield (WY), surface runoff
366 (SR), USLE soil erodibility factor (USLE_K), USLE agricultural practice factor
367 (USLE_P), slope, and the percentages of sand (Sand%), silt (Silt%) and clay
368 (Clay%) in soil. The input data to the PCA was the mean annual values of each
369 variable of 242 sub-basins. Results about soil erosion hot spots and triggering
370 factors are presented in section 3.4.

371 **3. RESULTS**

372 **3.1. SF under actual conditions**

373 3.1.1. Monthly variations of actual SF

374 Monthly and annual SF simulations and observations were plotted in Figure 4
375 and Figure 5, and their related statistics evaluations were reported in Table 3.
376 From the general performance ratings at monthly scale recommended by
377 Moriasi et al. (2007), Lao Cai, Yen Bai, Hoa Binh and Son Tay stations gained
378 good performance; Vu Quang station gained satisfactory performance. PBIAS
379 values indicate that the model slightly overestimated SF at most stations, and

underestimated SF at Hoa Binh station.

Table 3 Evaluation statistics of sediment flux (SF) on different time scales for each station from 2000 to 2013

Thanks to the satisfactory calibration of Q and SSC presented in Wei et al. (2019), simulated SF shows similar trends as observed SF and can be considered as satisfactory results (Figure 4). Base flow of simulated monthly SF fits well with observations at all stations.

SF shows great seasonal variations, especially in the Thao River (see stations of Lao Cai and Yen Bai in Figure 4). Maximum flux usually occurs from July to September, and minimum flux generally happens from February and March. 87-91% of the annual total SF was produced during the flood season (May to October). The ranges of monthly SF variations and the values of mean monthly SF for flood and dry seasons at each station were summarized in Table 4. The Thao sub-basin has the highest SF and specific sediment yield (SSY) compared to the other two sub-basins and to the whole Red River basin.

Table 4 Seasonal variation of sediment fluxes and mean monthly sediment fluxes for flood and dry seasons at five gauge stations

Figure 4. Observed (black dot) and simulated (gray solid line) monthly sediment flux, and simulated sediment flux of reference scenario (without dams, gray dash line) at five stations from 2000 to 2013.

3.1.2. Annual variations of actual SF

The annual SF exhibits different temporal and spatial variations among the 5 gauge stations (Figure 5). For the Thao River, the simulated annual SF ranged from 6.8 to 73.6 Mt yr^{-1} at Lao Cai (with 30.7 Mt yr^{-1} on average during 2000-2013, Table 5), and from 11.7 to 85.9 Mt yr^{-1} at Yen Bai (39.8 Mt yr^{-1} on average). The Lo River at Vu Quang is predicted to produce SF ranging from 2.0 to 12.5 Mt yr^{-1} (with 6.6 Mt yr^{-1} on average). On the Da River at Hoa Binh station, the minimum annual SF was 0.8 Mt yr^{-1} and the maximum was 7.1 Mt yr^{-1} (with 3.6 Mt yr^{-1} on average). Amongst these three tributaries, the Thao River produces the highest SF, followed by the Lo River, and the Da River generates the lowest SF. The Thao River shows higher SF than the other two tributaries due to its high SSC (the annual mean SSC during 2000-2013 at Lao Cai and Yen Bai were 1057 and 1003 mg L^{-1}, respectively, Wei et al., 2019). Even though SSC at Hoa Binh station on the Da River (the annual mean SSC during 2000-2013 was 57 mg L^{-1}, Wei et al., 2019) is much smaller than at Vu Quang on the Lo River (the annual mean SSC during 2000-2013 was 172 mg L^{-1}, Wei et al., 2019), the SF of these two rivers are in the same range. The Da River has a larger runoff (the annual mean Q during 2000-2013 was 1362 m^3 s^{-1}, Wei et al., 2019) with low SSC induced by dam retention, while the Lo River has a lower runoff (the annual mean Q during 2000-2013 was 729 m^3 s^{-1}, Wei et al., 2019) with a higher SSC. As the confluence of these tributaries, the Red River (at Son Tay station) yields an annual SF at the range of 8.0-69.2 Mt yr^{-1}, with an average specific sediment yield (SSY) of 240.3 t km^{-2} yr^{-1} over

426 2000-2013 (357.6 t km^{-2} yr^{-1} over 2000-2007 and 84.5 t km^{-2} yr^{-1} over
427 2008-2013).

428

429 Figure 5. Annual sediment flux (SF) variation from 2000-2013 at 5 gauge stations, and the mean annual
430 SF of pre-new-dams (2000-2007) and post-new-dams (2008-2013). The annual precipitation variation of
431 the whole basin from 2000-2013.

432 The values of mean annual SF during the study period and sub-periods from
433 references are displayed in Table 5. For the whole study period, simulated
434 mean annual SF shows a good match with in-situ data, though slight
435 overestimation at Yen Bai and Son Tay stations. By comparing the mean
436 annual SF of 2008-2013 between reference scenario and actual conditions,
437 the mean annual sediment trapped by the dams during this period ranged from
438 7.1 Mt yr^{-1} (Lo River) to 111.0 Mt yr^{-1} (Da River).

439 Table 5 Simulated sediment flux (Mt yr^{-1}) of reference scenario (without dams) and actual conditions (over the whole study period, 2000-2007 period and 2008-2013 period)
440 compared with other studies and in-situ data; values of trapped sediment (calculated as the difference between average values over 2008-2013 in the reference scenario and
441 actual simulations); impacts of short-term climate variability and dams.

442 AC†: Actual Conditions

443 RS‡: Reference Scenario (without dams)

3.2. SF of reference scenario (without dams)

3.2.1. Inter-annual variations

Like the actual SF (Figure 5), interannual SF of reference scenario (without dams) exhibits high variations. During the study period, results from reference scenario suggest that annual SF at Lao Cai, Yen Bai, Vu Quang and Hoa Binh stations should have been from 21.3 to 73.6 Mt yr^{-1}, 29.6 to 90.7 Mt yr^{-1}, 6.9 to 15.8 Mt yr^{-1}, 81.5 to 191.0 Mt yr^{-1}, respectively, thus with a factor of 3 between the highest and the lowest values in the Thao River, and a factor of 2.3 in the Lo and Da rivers. According to the results at the outlet (Son Tay station) the Red River basin should have exported 69.6 to 170.7 Mt yr^{-1} of sediment, with an average SSY of 778.8 t km^{-2} yr^{-1} over 2000-2013.

3.2.2. Mean annual SF

Annual SF of reference scenario was compared with observed data from references (Dang et al., 2010; Lu et al., 2015; Vinh et al., 2014, Table 5) which covered periods preceding the dams constructions, i.e. before 1979. Despite different periods, the simulations without dams for most stations (except Hoa Binh station) are close to those in-situ data. At Son Tay, the simulation without dams is slightly lower (~10%) than those reference data. These comparisons show that the model produces an acceptable simulation of SF without dams.

3.3. Simple Q-SF relationship under actual conditions

By using the outputs of the modelling, the simple relationships between Q and SF can be inferred at any point within the Red River and any temporal scales. As monthly mean Q data can be more easily accessed or gained, therefore, here we inferred the monthly mean Q-SF rating curves at the five gauge stations as an example.

For both the 2000-2007 and 2008-2013 periods, monthly simulated SF of actual conditions showed a positive power-law relation with monthly simulated Q for the 5 gauge stations as shown by fitted curves in Figure 6, with R^2 above 0.96. These 5 stations exported less SF after 2008, which highlights the changes caused by short-term climate variability and by sediment retention of dams. We, therefore, established separately power-law relationships between simulated Q and SF for both periods before and after 2008.

Figure 6. Correlation and relations between simulated monthly mean discharge (Q) and simulated monthly mean sediment fluxes (SF) at 5 stations in the simulation under actual conditions. Gray solid squares are of the period 2000-2007; gray hollow squares are of the period 2008-2013. Black solid and dash lines are the fitting curves of the period 2000-2007 and 2008-2013, respectively.

3.4. Hot spots of soil erosions

The SWAT model can not only be used to simulate, study and assess the in-stream SF, but also the sediment erosion from the land component. Then, based on these simulated mean annual sediment fluxes and soil erosion, hot spots of erosion were identified and presented in Figure 7c.

The model results indicate that the mean annual soil erosion in the whole basin ranged from 0.01 to 43.4 t ha^{-1} yr^{-1}, with a mean of 5.5 t ha^{-1} yr^{-1} (Figure 7c), and the mean annual soil erosion of the Red River basin during 2000-2013 was 64.0 Mt yr^{-1}. High erosion areas are identified in the middle part of the Thao River and the downstream of the Da River: with high precipitation (>1500 mm yr^{-1}, Figure 7a) and surface runoff (>450 mm yr^{-1}, Figure 7b), Lai Chau (sub-basin 173), Lao Cai (sub-basins 116, 117, 135, 148, 149, 157), Ha Giang (sub-basin 119) and Son La (sub-basins 218, 232, 234, 237, 240, 241) provinces are the most vulnerable to soil erosion, and their mean annual erosion rate during the study period can be above 20 t ha^{-1}.

Figure 7d presents the in-stream SF spatial variations. High SF can reach locally above 80 t yr^{-1}, with hot spots of high values identified upstream of the Hoa Binh dam, which corresponds with the annual SF values before Hoa Binh dam construction (Table 5).

Figure 7. Mean annual value of (a) Precipitation distribution (mm yr^{-1}), (b) Surface Runoff (mm yr^{-1}), (c) Soil Erosion (ton ha^{-1} yr^{-1}), (d) In-stream Sediment Flux (ton yr^{-1}) within 242 sub-basins, derived from the actual conditions simulation over the period 2000-2013.

Principal component analysis (PCA) was applied to identify the factors influencing soil erosion (Table 6). The PCA results based on the correlation matrix analysis with Varimax rotation produce 3 principal components (PCs) with eigenvalues greater than 1.00, corresponding to an overall cumulative variance of 78.3%, moreover, the 2 first PCs represent a cumulated variance of

509 67.5%.

510 Table 6 The principal component (PC) loading

511 †: the simulation from the model

512 ‡: the observation and input data

513 Notes: underlined values correspond to the first three highest factor loadings in the PC.

514

515 **4. DISCUSSION**

516 **4.1. Uncertainties**

517 Differences between simulations and observations are large on some peaks of
518 SF flow: during these peaks, the SF can be underestimated by a factor >2
519 (Figure 4). Uncertainties can come from three factors: uncertainties associated
520 with rainfall satellite input data; errors due to the numerical simulation
521 approximations; uncertainties associated with in-situ measurement errors on Q
522 and SSC.

523 Previous studies indicated that the TRMM (satellite rainfall dataset)
524 underestimated the rainfall when there were intensive or extreme rainfall
525 events (Le et al., 2014; Liu et al., 2015; Simons et al., 2016). The
526 underestimations on rainfall values can cause underestimations in Q
527 simulation which might induce underestimations in channel erosion and
528 re-suspended processes (Wei et al., 2019) and also in soil erosion.

529 Some studies indeed showed that modelling might underestimate SSC during
530 high and intensive rainfall (Oeurng et al., 2011; Xu et al., 2009). Modelling

errors can come from the simplification of algorithms. For example, in SWAT, for land erosion SWAT model uses a runoff factor instead of rainfall energy factor (Equation 1); and for the channel processes, SWAT uses a simplified version of Bagnold stream power equation to calculate the maximum amount of sediment that could be transported in a stream segment (Equation 2, Bagnold, 1977; Neitsch et al., 2009). However, this algorithm does not keep track of particle size distribution of elements that pass through the channel, and sediments all are assumed to be of silt size. Besides, the channel erosion is not partitioned between stream bank and bed, and deposition is assumed to occur only in the main channel; flood plain sediment deposition is also not modelled separately (Neitsch et al., 2009). Therefore, this simplification can cause deviations for sediment routing.

In-situ measurements and sampling strategy can also cause errors. For example, a high sampling frequency enables to diminish errors in the estimation of annual SF (Dang et al., 2010). Q and SSC measurements during flood events are usually extrapolated by the rating curve. However, the fact that those rating curves may have been established based on non-exceptional conditions might cause deviations on both Q and SSC, and consequently on SF.

Besides the above main factors, irrigation diversion and sand excavation can also affect suspended sediment transfer. However, no available data to quantify their impacts on SF of the Red River. Future studies should fill this gap.

554 **4.2. SF variations caused by short-term climate variability**

555 Comparing the annual SF of reference scenario (without dams) between
556 2008-2013 and 2000-2007 shows that short-term climate variability has
557 different impacts on these tributaries, though it induces a decrease at most
558 stations, except at Vu Quang (Table 5 and Figure 5). The biggest impacts are
559 observed at the two stations on the Thao River (Lao Cai and Yen Bai), causing
560 an average 25% decrease of SF, followed by the Da River (Hoa Binh, ~-10%),
561 with a resulting ~10% decrease on the Red River (Son Tay). On the contrary,
562 at Vu Quang station, the mean annual SF very slightly increased by 2%, in
563 accordance with a similar Q change (2%, Wei et al., 2019).

564 In order to figure out the different responses of each tributary to short-term
565 climate variability, we compared the rainfall and water availability (the
566 difference between rainfall and evapotranspiration) variations between
567 2008-2013 and 2000-2007, and the variations are presented in Figure 8. In the
568 upper and middle parts of the Red River basin, both rainfall and water
569 availability decreased while the lower part showed an increasing tendency. At
570 sub-basin scale, the variations of the rainfall were -9% for the Thao basin, +2%
571 for the Lo basin and -2% for the Da basin; for water availability, the Thao and
572 Da basins decreased by 13% and 4%, respectively, while the Lo basin
573 increased by 7%. The impacts of short-term climate variability on SF for each
574 sub-basin are in accordance with the variations of rainfall and
575 evapotranspiration: the Thao river showed the largest reduction while the Lo
576 river showed an increase.

577 Previous studies revealed that climate variability had an effect on both Q and
578 SSC in the Red River basin (Wei et al., 2019), and suggested a decrease of
579 rainfall mean and extremes over the last decades over Southeast Asia
580 (Manton et al., 2001). A 14-year period is not long enough for detecting the
581 climate variability on SF, therefore, this study only aimed at discovering the
582 different responses of each subbasin to the short-term climate variability during
583 the study period, and does not make conclusions for climate changes and the
584 tendency for the future. Longer periods of study are needed to study the
585 climate trends and variability effects on SF. The SF trend of the Red River
586 under the influence of long-term climate variability and hydrology changes will
587 be carried out in future studies based on the methodology proposed by this
588 study.

589

590 Figure 8. The differences in annual rainfall (a) and annual water availability (b) between 2008-2013 and
591 2000-2007.

592 **4.3. Impacts of dams**

593 4.3.1. The reduction caused by dams

594 Among the three tributaries, dams' impact on the outlet of the Da River (Hoa
595 Binh station) is the most severe, followed by the Lo River; and the dams are
596 less affected on the Thao River (Table 5). Two new dams in China caused
597 around a 48% reduction of SF on the Thao River. More cascade dams are
598 under construction in China, so this value can provide a reference for future

599 studies. The dams on the Lo River reduced around 74% of the annual SF. The
600 large dams on the Da River show an enormous impact on SF, and the trap
601 efficiency is 89% compared to 86-91% from other studies which did not
602 estimate the specific impacts of climate variations of different periods and
603 neither the impact of the Son La dam (Dang et al., 2010; Vinh et al., 2014). At
604 the outlet of the Red River basin, the dams upstream caused an 80% decrease
605 of annual SF.

606 The Son La and Hoa Binh dams on the Da River have large capacities and are
607 located quite downstream to the outlet of the river compared to the dams on
608 the other two tributaries, explaining their higher relative impact. The capacities
609 of the Thac Ba and Tuyen Quang dams are also larger than the two dams on
610 the Thao River. The two dams (Nansha and Madushan) on the Thao River are
611 above 100 km upstream of the Yen Bai station, and along the reach between
612 the dams and Yen Bai station, the impacts of dams on sediment transport are
613 mitigated by the degradation and the soil erosion from the land component.
614 Therefore, the dams show larger impact at the outlet of the Lo River than the
615 Thao River.

616 Previous studies (Dang et al., 2010; Lu et al., 2015; Vinh et al., 2014) used
617 long-term observed Q and SSC data to analyse the impact of dams on SF.
618 Dang et al. (2010) analysed the observed Q and SSC from 1960-2008, but
619 only at Son Tay station, did not study the Lo and the Da rivers; Vinh et al. (2014)
620 analysed the observed data from 1960-2010 at four stations (not in Lao Cai)
621 and focused the analysis on the impact of the Hoa Binh dam; Lu et al. (2015)

622 also used the observed data from 1960-2010 to assess the impact of a
623 sequence of dams but without considering the dams upstream in China. This
624 study revisits the impacts of dams by taking into account more dams recently
625 built in the Red River basin. With more dams implemented after 2013 or
626 planned at short/mid-term on these three tributaries, the sediment trap
627 efficiency might still increase and the SF decreases at the outlet of each
628 tributary, consequently at the outlet of the Red River.

629 4.3.2. Impacts on dynamic processes

630 From the seasonal variation of SF (Figure 4), it can be noticed that the flow
631 curve (dynamic processes) with and without dams are similar; the impacts of
632 dams are significant on SF peak flow during flood seasons, and dams have
633 much fewer impacts on the base flow of SF.

634 However, the impacts on the dynamic processes at each station can be
635 different. For example, in 2008, the simulation without dams seems to fit the
636 observations better at Yen Bai and Vu Quang than at other stations. This
637 suggests that, on the same river (Thao), the Nansha dam had weaker impacts
638 at Yen Bai (located more downstream, Figure 1) than at Lao Cai for the first
639 year of dam operation, and it can be related to the sediment degradation
640 processes between Lao Cai and Yen Bai. Also, the Tuyen Quang dam only
641 slightly impacted SF at Vu Quang for the first year of implementation,
642 presumably because the Lo River has much less SS than the other two
643 tributaries and the sediment retention caused by the new dam at the first year

644 can be relatively lighter. Besides, the Tuyen Quang dam is located on one
645 tributary of the Lo River, whereas the other dams are located directly in the
646 main branch of the Thao and Da rivers. Therefore, the Tuyen Quang dam on
647 the Lo River has smaller impacts on sediment transport. In addition, the
648 operation scheme of these new dams can be also a reason that induces
649 different impacts on SS dynamic processes as different discharge releases
650 can carry different amounts of sediment, and discharge release of each dam
651 depends on the main function (flood control or irrigation or power generation)
652 of this dam and its capacity (Wang et al., 2017).

653 **4.4. Soil erosion**

654 The PCA results identified the factor loadings of each component (Table 6):
655 PC1 (consisted of precipitation (P), water yield (WY) and surface runoff (SR))
656 has the highest weighted variable (41.6%), followed by PC2 (25.9%) which is
657 consisted of soil erosion (SE), slope and USLE agricultural practice factor
658 (USLE_P), and PC3 (10.8%, the percentage of sand (Sand%), silt (Silt%) and
659 clay (Clay%) in soil, i.e. the soil texture). Therefore, precipitation (as water
660 yield and surface runoff are fractions of precipitation), slope and USLE
661 agricultural practice factor (USLE_P) are key influence factors for soil erosion
662 in the Red River basin. The soil texture is also a significant factor. Our results
663 are in agreement with He et al. (2007) who indicated that human activities and
664 climate change are the major influences to the sediment change in the
665 mountainous upstream area in China and Ranzi et al. (2012) who highlighted
666 the major role of rainfall in soil erosion in the Lo basin; Yang et al. (2003) found

667 that the hot spots of soil erosion in Southeast Asia were close mountainous
668 areas located in the tectonic zones and dense croplands regions where both
669 natural geomorphology and human activity are major factors for inducing soil
670 erosion. In the middle part of the Ren River basin (especially in the Thao and
671 Da subbasins), agricultural activities are distributed in these mountain areas
672 with steep slopes, and terrace systems and contour farming are popular.
673 Therefore, in these hot spots of soil erosion, agricultural practices on steep
674 mountain areas should be paid attention. With more forests might be
675 converted to farmland in the future, soil erosion might be increased.

676 In the upper Red River basin in China, the soil erosion area accounted for ~44%
677 of the total basin area in China, with a soil modulus of 14.8 t ha^{-1} yr^{-1} (He et al.,
678 2007). Tuan et al. (2014) found annual soil losses from 1.8 to 174 t ha^{-1} yr^{-1}
679 from plot-scale experiment near Son La. Podwojewski et al. (2008) found a soil
680 erosion from 0.86 to 13.5 t ha^{-1} yr^{-1} also in Hoa Binh province on steep slopes.
681 Based on a RUSLE model, Nguyen et al. (2012) simulated a continuous
682 increase of the soil erosion from 1970 to the recent decade 2000, from 4.9 to
683 5.9 t ha^{-1} yr^{-1}. Mai et al. (2013) found a 1.63 to 17.22 t ha^{-1} yr^{-1} erosion rate
684 near Son Tay. Our simulation is in the range of these references: from 0.01 to
685 43.4 t ha^{-1} yr^{-1}, with a mean of 5.5 t ha^{-1} yr^{-1} over the whole basin.

686 The soil of the high erosion areas - the middle part of the Thao River and the
687 downstream of the Da River (Figure 7c) - is mainly composed of Orthic Acrisols
688 (Ao90-2-3c-4284, Figure 2c and Table S-3). This type of soil is acid with
689 sandy-loamy surface soil, and prone to slaking, crusting and erosion. Acrisols

690 form the tropical red soils and red earths, and after eluviation they are
691 subjected to erosion (FAO, 2003). This result is in agreement with the above
692 conclusion obtained from PCA.

693 Estimates of annual SF show that Yen Bai produces more SF than Lao Cai
694 (~30% over the whole period, both under reference scenario and actual
695 conditions, Figure 5). This indicates that the soil erosion or/and resuspension
696 likely happens in the part of the basin between Lao Cai and Yen Bai. This can
697 be confirmed by the spatial identification of soil erosion (Figure 7c) which also
698 indicates that Lao Cai province is a hot spot of soil erosion.

699 Before the construction of Hoa Binh dam, sediment input to the Red River
700 mainly originated from the Da River (~120 Mt yr^{-1} in the reference scenario
701 simulations, i.e. more than twice the values estimated for the other tributaries,
702 Table 5). The high in-stream SF of the Da River results from both land erosion
703 and channel degradation. Complex dam regulation can cause complex
704 hydraulics compared to the natural channel. Comparison of the reference
705 scenario (without dams) and actual conditions simulations over the period
706 2008-2013 suggests a 111 Mt yr^{-1} value of trapped sediment at the Hoa Binh
707 dam. Such a big quantity of sediment from upstream of Hoa Binh should catch
708 the attention of the management because big sedimentation in the reservoir
709 would reduce the capacity and performance of the dam. As explained in
710 section 2.1.4, this is also a reason why the Son La dam was built.

711 **4.5. Comparison with other basins**

712 To compare our results with SF and specific sediment yield (SSY) without
713 dams obtained for other Asian rivers, the values provided by Milliman and
714 Syvitski (1992) were considered since they were obtained before 1992 and are
715 less impacted by dams than more recent estimates provided by the literature.
716 From our simulation of reference scenario (without dams), the Red River yields
717 an annual SF of 107 Mt yr^{-1}, corresponding to a SSY of 780 t km^{-2} yr^{-1} (Table 5).
718 The Yellow River produced 1100 Mt yr^{-1} SF with a SSY of 1400 t km^{-2} yr^{-1}; the
719 Yangtze River caused 480 Mt yr^{-1} SF with a SSY of 250 t km^{-2} yr^{-1}; the Pearl
720 River generated 69 Mt yr^{-1} SF with a SSY of 160 t km^{-2} yr^{-1}; the Mekong River
721 yielded 160 Mt yr^{-1} SF with a SSY of 200 t km^{-2} yr^{-1} (Milliman and Syvitski,
722 1992). The Red River basin without dams thus exported less SF than the
723 Yellow River (-90%), the Yangtze River (-78%) and the Mekong River (-33%),
724 and 55% more than the Pearl River. However, its SSY was higher than the
725 Mekong (+290%), Pearl River (+388%), Yangtze (+212%), and nearly half of
726 the Yellow River (-44%). When compared to an equivalent surface watershed
727 such as the upper Danube (132,000 km^2), the Red River basin produced
728 almost 3 times higher SSY than that of 265 t km^{-2} yr^{-1} generated by the upper
729 Danube; besides, the upper Danube basin only exported 21.2 t km^{-2} yr^{-1} to the
730 downstream part (Vigiak et al., 2015). These results show that without impacts
731 of dams, the Red River basin, though having a smaller surface than the other
732 basins in the world, would be a very large source of suspended sediments to
733 the sea due to its soil erosion caused by active tectonic movements, steep

734 slopes, deep valleys, high precipitation and intensive agricultural activities
735 along the upstream river (Le et al., 2017, 2007).

736 **4.6. Interpretation of Q-SF simple relations**

737 From Figure 6, we can see that the relation between monthly Q and SF is a
738 power-law relation of the form:

739 $$\mathrm{SF} = \mathrm{a}Q^{b}$$

740 (3)

741 where SF is the monthly mean sediment flux (t day^{-1}), Q is monthly mean water
742 discharge (m^3 s^{-1}), *a* and *b* are regression coefficients.

743 Equation (3) is formally in accordance with a general sediment rating curve
744 (Asselman, 2000; Syvitski et al., 2000):

745 $$\mathrm{SSC} = a'Q^{b'}$$

746 (4)

747 where SSC is the suspended sediment concentration (mg L^{-1}), *a'* and *b'* being
748 the regression coefficients. The coefficient *a'* represents the erodibility of the
749 soil, and is equal to SSC when Q is 1 m^3 s^{-1}; a sub-basin with intensively
750 weathered materials which can be eroded and transported easily usually
751 shows a high value of the coefficient *a'*. The coefficient *b'* represents the
752 erosive power of the river and the transport capacity; it is also affected by the
753 grain size distribution of the material available for transport: rivers with
754 sand-sized sediments have higher *b'* values than rivers with silt and clay-sized

sediments.

As discussed before, among the three sub-basins, the Thao and Da sub-basins present steep slopes and are vulnerable to soil erosion, therefore their *a*-coefficient should be high. The two stations on the Thao River have the highest *a* values (Figure 6); however, the Hoa Binh station on the Da River has the lowest *a* value among these three tributaries because the eroded soil was retained in the Hoa Binh dam. For each station, the *a*-value decreased between 2000-2007 and 2008-2013 (Figure 6): dams retain the SS from upstream soil erosion which induces a decrease of *a* value downstream of the dam.

The average values of the median diameter D_{50} of surface sediment before new dam constructions are 0.16, 0.35, 0.175 and 0.2 mm in the Thao, Da, Lo rivers and the reach between the confluence of the Da and Thao rivers at Son Tay, respectively (Vinh et al., 2014), and there is a relationship between the parameter *b* (over the period 2000-2007, before new dams) and the values of the median diameter D_{50} of surface sediment before new dam constructions (Figure 9). The *b* values during 2000-2007 are similar at Lao Cai and Yen Bai on the Thao river and at Vu Quang on the Lo river (from 1.61 to 1.65, Figure 6), but not during 2008-2013 (1.79 at Lao Cai and Yen Bai vs.1.59 at Vu Quang). The differences of the b values between 2000-2007 and 2008-2013 can indicate that the dams on the Thao and Lo rivers might change the grain size distributions and transport capacity at these stations: new dam constructions may have induced a higher (with *b* increasing) median diameter D_{50} of surface

778 sediment in the Thao river while a lower one (with *b* decreasing) in the Lo river.

779

780 Figure 9. Relationship between the parameter *b* and the values of the median diameter D50 of surface
781 sediment

782 The coefficients *a* and *b* in the simple Q-SF equation are in agreement with the
783 real sub-basin characteristics. The curves of two periods also illustrate the
784 differences of the sediment regimes during these two periods: curves of
785 2008-2013 are gentler than of 2000-2007 (Figure 6), i.e. under the same Q, the
786 SF is lower compared to 2000-2007, which is due to a combined impact of
787 climate and dams. Also, the outputs from the model can be used to infer Q-SF
788 relationship at any other point within this basin. Hence, these simple Q-SF
789 equations can be used by stakeholders to estimate the monthly SF without
790 using the SWAT model.

791 **5. CONCLUSIONS**

792 This study aimed to characterize the suspended sediment flux and the soil
793 erosion of the Red River basin by using the outputs of a numerical model and
794 in-situ data. Suspended sediment flux was quantified based on daily
795 simulations of discharge and suspended sediment concentration during a long
796 period, taking into account the successive implementations of dams and the
797 short-term climate variability during this period. Furthermore, by implementing
798 a reference scenario (without dams in this basin), this study allowed to
799 disentangle the impacts of short-term climate variability and damming at the

800 outlets of each main tributary as well as at the outlet of the continental basin.
801 This provides a reference for future studies on dams' functions and water
802 resource management.

803 Under the main influence of damming, the suspended sediment fluxes showed
804 a drastic decrease during 2008-2013 compared to 2000-2007. These two
805 influencing factors had different effects on each sub-basin. Due to the different
806 climatic characteristics, such as precipitation distribution and variation, the
807 Thao River is more sensitive to short-term climate variability than the other two
808 tributaries. Conversely, the Da River is the most affected by constructions of
809 huge-capacity dams. At the outlet of the Red River basin, the mean annual
810 sediment fluxes decreased by 90% compared to the value estimated from
811 reference scenario (without dams) during 2000-2007, of which 10% was due to
812 short-term climate variability and 80% to the dams. A power-law relation
813 between monthly mean discharge and sediment flux was provided at each
814 outlet of the main tributaries and the Red River for stakeholders and
815 decision-makers to have an easy tool to estimate the sediment flux.

816 The high advantage of the model, once it has been calibrated with data from
817 hydrological stations, is that it can serve to estimate and map each term
818 involved in the sediment transport process – including local erosion, local
819 deposition, in-stream sediment discharge, etc. – and that it can be used to infer
820 local SF-Q rating curves at any virtual station within the basin from the model
821 simulations, even where there is no true station. This point is of major interest
822 both for scientific applications (e.g., studying spatial variations of SF) and for

823 management purposes, with provinces and other stakeholders.

824 Land management (such as agricultural practice) should pay attention on the
825 high soil erosion areas located in the middle part of the Thao sub-basin and the
826 lower part of the Da sub-basin due to the precipitation distribution, topography
827 and soil texture, and river management should notice the sediment retained in
828 the dams on the Da River.

829 Some improvements can be done in future research. This study hypothesized
830 that the impact of the land use changes was not significant during our study
831 period and did not take into account the impacts of land use changes on soil
832 erosion and sediment flux. In the future, more forests might be converted into
833 farmland in this basin, therefore, it would be interesting to evaluate the impacts
834 of land use change on sediment fluxes. A more precise and higher-frequency
835 in-situ dataset would be useful, such as longer and high-frequency
836 hydrological and meteorological data at more stations, and more information
837 about dam management, in order to have a better estimation and
838 understanding of the impacts of climate variability and human interferences.

839 With on-going and future climate change and dam constructions in this basin, it
840 would be necessary to pursue further research about the sediment flux
841 variation and its associated contaminant fluxes as well as carbon transfer in
842 order to better manage this basin and protect the downstream coastal areas. In
843 addition, running numerical simulations under scenarios of global changes,
844 such as land use changes and urbanization, would allow us to estimate the

impacts of these changes on hydrology and suspended sediment fluxes.

ACKNOWLEDGEMENT:

This research was developed in the framework of the Land-Ocean-aTmosphere regional coUpled System study center (LOTUS), an international joint Vietnamese/French laboratory (http://lotus.usth.edu.vn/) funded by the Institut de Recherche pour le Développement (IRD). We thank LOTUS for providing the dataset, and also the research travel funds for Xi Wei to collect data and information in Vietnam. The PhD scholarship of Xi Wei is financially supported by the China Scholarship Council (CSC), grant number 201606240088.

CONFLICTS OF INTEREST:

The authors declare that no conflict of interest could be perceived as prejudicing the impartiality of the research reported.

References:

Arias, M.E., Cochrane, T.A., Kummu, M., Lauri, H., Holtgrieve, G.W., Koponen, J., Piman, T., 2014. Impacts of hydropower and climate change on drivers of ecological productivity of Southeast Asia's most important wetland. Ecol. Modell. 272, 252–263. https://doi.org/10.1016/j.ecolmodel.2013.10.015

Arnold, J.G., Srinivasan, R., Muttiah, R.S., Williams, J.R., 1998. Large area hydrologic modeling and assesment Part I: Model development. JAWRA J. Am. Water Resour. Assoc.

34, 73–89. https://doi.org/10.1111/j.1752-1688.1998.tb05961.x

Asselman, N.E.M., 2000. Fitting and interpretation of sediment rating curves. J. Hydrol. 234, 228–248. https://doi.org/10.1016/S0022-1694(00)00253-5

Bagnold, R.A., 1977. Bed load transport by natural rivers. Water Resour. Res. 13, 303–312. https://doi.org/10.1029/WR013i002p00303

Bai, Z., Feng, D., Ding, J., Duan, X., 2015. A study on the variations of soil physico-chemical properties and its environmental impact factors in the Red River watershed (in Chinese). Yunnan Geogr. Environ. Res. 27, 81–90. https://doi.org/10.13277/j.cnki.jcwu.2015.04.013

Barton, A.P., Fullen, M.A., Mitchell, D.J., Hocking, T.J., Liu, L., Wu Bo, Z., Zheng, Y., Xia, Z., 2004. Effects of soil conservation measures on erosion rates and crop productivity on subtropical Ultisols in Yunnan Province, China. Agric. Ecosyst. Environ. 104, 343–357. https://doi.org/10.1016/j.agee.2004.01.034

Basilevsky, A., 1994. Statistical Factor Analysis and Related Methods-Chapter 3: The Ordinary Principal Components Model, Wiley Series in Probability and Statistics. John Wiley & Sons, Inc., Hoboken, NJ, USA. https://doi.org/10.1002/9780470316894

Beusen, A.H.W., Van Beek, L.P.H., Bouwman, A.F., Mogollón, J.M., Middelburg, J.J., 2015. Coupling global models for hydrology and nutrient loading to simulate nitrogen and phosphorus retention in surface water - Description of IMAGE-GNM and analysis of performance. Geosci. Model Dev. 8, 4045–4067. https://doi.org/10.5194/gmd-8-4045-2015

Chen, J., Shi, H., Sivakumar, B., Peart, M.R., 2016. Population, water, food, energy and dams. Renew. Sustain. Energy Rev. 56, 18–28. https://doi.org/10.1016/j.rser.2015.11.043

Cohen, S., Kettner, A.J., Syvitski, J.P.M., 2014. Global suspended sediment and water discharge dynamics between 1960 and 2010: Continental trends and intra-basin sensitivity. Glob. Planet. Change 115, 44–58. https://doi.org/10.1016/j.gloplacha.2014.01.011

Dai, S.B., Yang, S.L., Li, M., 2009. The sharp decrease in suspended sediment supply from China's rivers to the sea: Anthropogenic and natural causes. Hydrol. Sci. J. 54, 135–146. https://doi.org/10.1623/hysj.54.1.135

Dang, T.H., Coynel, A., Orange, D., Blanc, G., Etcheber, H., Le, L.A., 2010. Long-term monitoring (1960-2008) of the river-sediment transport in the Red River Watershed (Vietnam): Temporal variability and dam-reservoir impact. Sci. Total Environ. 408, 4654–4664. https://doi.org/10.1016/j.scitotenv.2010.07.007

Dang, T.H., Ouillon, S., Van Vinh, G., 2018. Water and Suspended Sediment Budgets in the Lower Mekong from High-Frequency Measurements (2009–2016). Water 10, 846. https://doi.org/10.3390/w10070846

Dile, Y.T., Srinivasan, R., 2014. Evaluation of CFSR climate data for hydrologic prediction in data-scarce watersheds: an application in the Blue Nile River Basin. JAWRA J. Am. Water Resour. Assoc. 50, 1226–1241. https://doi.org/10.1111/jawr.12182

FAO, 2011a. The state of the world's land and water resources for food and agriculture (SOLAW) – Managing systems at risk, Food and Agriculture Organization of the United Nations, Rome and Earthscan, London. Food and Agriculture Organization of the United Nations, Rome and Earthscan, London.

FAO, 2011b. Irrigation in Southern and Eastern Asia in figures, AQUASTAT Survey – FAO Water report 37.

FAO, 2003. Multilingual Thesaurus on Land Tenure (Chinese version).

Furuichi, T., Win, Z., Wasson, R.J., 2009. Discharge and suspended sediment transport in the Ayeyarwady River, Myanmar: centennial and decadal changes. Hydrol. Process. 23, 1631–1641. https://doi.org/10.1002/hyp.7295

Hauer, C., Leitner, P., Unfer, G., Pulg, U., Habersack, H., Graf, W., 2018. The Role of Sediment and Sediment Dynamics in the Aquatic Environment, in: Riverine Ecosystem Management. Springer International Publishing, Cham, pp. 151–169.

https://doi.org/10.1007/978-3-319-73250-3_8

He, D., Ren, J., Fu, K., Li, Y., 2007. Sediment change under climate changes and human activities in the Yuanjiang-Red River Basin. Chinese Sci. Bull. 52, 164–171. https://doi.org/10.1007/s11434-007-7010-8

Hiep, N.H., Luong, N.D., Viet Nga, T.T., Hieu, B.T., Thuy Ha, U.T., Du Duong, B., Long, V.D., Hossain, F., Lee, H., 2018. Hydrological model using ground- and satellite-based data for river flow simulation towards supporting water resource management in the Red River Basin, Vietnam. J. Environ. Manage. 217, 346–355. https://doi.org/https://doi.org/10.1016/j.jenvman.2018.03.100

IPCC, 2019. Special Report on climate change, desertification, land degradation, sustainable land management, food security, and greenhouse gas fluxes in terrestrial ecosystems. The Intergovernmental Panel on Climate Change. Geneva, Switzerland.

Jiang, T., Fischer, T., Lu, X., 2009. Larger Asian rivers: Climate change, river flow, and watershed management. Quat. Int. 208, 1–3. https://doi.org/10.1016/j.quaint.2010.06.011

Khoi, D.N., Suetsugi, T., 2014. The responses of hydrological processes and sediment yield to land-use and climate change in the Be River Catchment, Vietnam. Hydrol. Process. 28, 640–652. https://doi.org/10.1002/hyp.9620

Kunz, M.J., Wüest, A., Wehrli, B., Landert, J., Senn, D.B., 2011. Impact of a large tropical reservoir on riverine transport of sediment, carbon, and nutrients to downstream wetlands. Water Resour. Res. https://doi.org/10.1029/2011WR010996

Lal, R., Kimble, J., Levine, E., Stewart, B.A., 1995. Soils and global change. CRC Press, Boca Raton, USA.

Lauri, H., Räsänen, T.A., Kummu, M., 2014. Using Reanalysis and Remotely Sensed Temperature and Precipitation Data for Hydrological Modeling in Monsoon Climate: Mekong River Case Study. J. Hydrometeorol. 15, 1532–1545. https://doi.org/10.1175/JHM-D-13-084.1

945 Le, T.B., Al-Juaidi, F.H., Sharif, H., 2014. Hydrologic simulations driven by satellite rainfall to
946 study the hydroelectric development impacts on river flow. Water (Switzerland) 6, 3631–
947 3651. https://doi.org/10.3390/w6123631

948 Le, T.P.Q., 2005. Biogeochemical Functioning of the Red River (North Vietnam): Budgets and
949 Modelling. Université Paris VI- Pierre et Marie Curie.

950 Le, T.P.Q., Dao, V.N., Rochelle-Newall, E., Garnier, J., Lu, X., Billen, G., Duong, T.T., Ho, C.T.,
951 Etcheber, H., Nguyen, T.M.H., Nguyen, T.B.N., Nguyen, B.T., Da Le, N., Pham, Q.L., 2017.
952 Total organic carbon fluxes of the Red River system (Vietnam). Earth Surf. Process.
953 Landforms 42, 1329–1341. https://doi.org/10.1002/esp.4107

954 Le, T.P.Q., Garnier, J., Gilles, B., Sylvain, T., Van Minh, C., 2007. The changing flow regime and
955 sediment load of the Red River, Viet Nam. J. Hydrol. 334, 199–214.
956 https://doi.org/10.1016/j.jhydrol.2006.10.020

957 Le, T.P.Q., Le, N. Da, Dao, V.N., Rochelle-Newall, E., Nguyen, T.M.H., Marchand, C., Duong,
958 T.T., Phung, T.X.B., 2018. Change in carbon flux (1960–2015) of the Red River (Vietnam).
959 Environ. Earth Sci. 77, 658. https://doi.org/10.1007/s12665-018-7851-2

960 Lehner, B., Liermann, C.R., Revenga, C., Vörösmarty, C., Fekete, B., Crouzet, P., Döll, P.,
961 Endejan, M., Frenken, K., Magome, J., Nilsson, C., Robertson, J.C., Rödel, R., Sindorf, N.,
962 Wisser, D., 2011. High-resolution mapping of the world's reservoirs and dams for
963 sustainable river-flow management. Front. Ecol. Environ. 9, 494–502.
964 https://doi.org/10.1890/100125

965 Lever, J., Krzywinski, M., Altman, N., 2017. Principal component analysis. Nat. Methods 14,
966 641–642. https://doi.org/10.1038/nmeth.4346

967 Li, X., Li, Y., He, J., Luo, X., 2016. Analysis of variation in runoff and impacts factors in the
968 Yuanjiang-Red River Basin from 1956 to 2013. Resour. Sci. (in Chinese) 38, 1149–1159.
969 https://doi.org/10.18402/resci.2016.06.14

970 Li, Y., He, D., Ye, C., 2008. Spatial and temporal variation of runoff of red river basin in Yunnan.

J. Geogr. Sci. 18, 308–318. https://doi.org/10.1007/s11442-008-0308-x

Li, Y., He, J., Li, X., 2016. Hydrological and meteorological droughts in the Red River Basin of Yunnan Province based on SPEI and SDI Indices (In Chinese). Prog. Geogr. 35, 758–767.

Liu, J., Duan, Z., Jiang, J., Zhu, A.-X., 2015. Evaluation of Three Satellite Precipitation Products TRMM 3B42, CMORPH, and PERSIANN over a Subtropical Watershed in China. Adv. Meteorol. 2015, 1–13. https://doi.org/10.1155/2015/151239

Lu, X.X., Oeurng, C., Le, T.P.Q., Thuy, D.T., 2015. Sediment budget as affected by construction of a sequence of dams in the lower Red River, Viet Nam. Geomorphology 248, 125–133. https://doi.org/10.1016/j.geomorph.2015.06.044

Ludwig, W., Probst, J.L., 1996. Predicting the oceanic input of organic carbon by continental erosion. Global Biogeochem. Cycles 10, 23–41. https://doi.org/10.1029/95GB02925

Luu, T.N.M., Garnier, J., Billen, G., Orange, D., Némery, J., Le, T.P.Q., Tran, H.T., Le, L.A., 2010. Hydrological regime and water budget of the Red River Delta (Northern Vietnam). J. Asian Earth Sci. 37, 219–228. https://doi.org/10.1016/j.jseaes.2009.08.004

Mai, V.T., van Keulen, H., Hessel, R., Ritsema, C., Roetter, R., Phien, T., 2013. Influence of paddy rice terraces on soil erosion of a small watershed in a hilly area of Northern Vietnam. Paddy Water Environ. https://doi.org/10.1007/s10333-012-0318-2

Manton, M.J., Della-Marta, P.M., Haylock, M.R., Hennessy, K.J., Nicholls, N., Chambers, L.E., Collins, D.A., Daw, G., Finet, A., Gunawan, D., Inape, K., Isobe, H., Kestin, T.S., Lefale, P., Leyu, C.H., Lwin, T., Maitrepierre, L., Ouprasitwong, N., Page, C.M., Pahalad, J., Plummer, N., Salinger, M.J., Suppiah, R., Tran, V.L., Trewin, B., Tibig, I., Yee, D., 2001. Trends in extreme daily rainfall and temperature in Southeast Asia and the South Pacific: 1961-1998. Int. J. Climatol. 21, 269–284. https://doi.org/10.1002/joc.610

Milliman, J.D., Meade, R.H., 1983. World-wide delivery of river sediment to the oceans. J. Geol. 91. https://doi.org/10.1086/628741

997 Milliman, J.D., Syvitski, J.P.M., 1992. Geomorphic/Tectonic Control of Sediment Discharge to
998 the Ocean: The Importance of Small Mountainous Rivers. J. Geol. 100, 525–544.
999 https://doi.org/10.1086/629606

1000 Moriasi, D.N., Arnold, J.G., Van Liew, M.W., Bingner, R.L., Harmel, R.D., Veith, T.L., 2007.
1001 Model Evaluation Guidelines for Systematic Quantification of Accuracy in Watershed
1002 Simulations. Trans. ASABE 50, 885–900. https://doi.org/10.13031/2013.23153

1003 Neitsch, S.., Arnold, J.., Kiniry, J.., Williams, J.., 2009. Soil and Water Assessment Tool
1004 Theoretical Documentation Version 2009. Texas Water Resour. Inst.
1005 https://doi.org/10.1016/j.scitotenv.2015.11.063

1006 Nguyen, V.T., Orange, D., Laffly, D., Pham, V.C., 2012. Consequences of large hydropower
1007 dams on erosion budget within hilly agricultural catchments in Northern Vietnam by
1008 RUSLE modeling, in: International Conference Sediment Transport Modeling in
1009 Hydrological Watersheds and Rivers. Istanbul, Turkey, pp. 14–16.

1010 Oeurng, C., Sauvage, S., Sánchez-Pérez, J.M., 2011. Assessment of hydrology, sediment and
1011 particulate organic carbon yield in a large agricultural catchment using the SWAT model. J.
1012 Hydrol. 401, 145–153. https://doi.org/10.1016/j.jhydrol.2011.02.017

1013 Ouillon, S., 2018. Why and how do we study sediment transport? Focus on coastal zones and
1014 ongoing methods. Water (Switzerland) 10. https://doi.org/10.3390/w10040390

1015 Peng, J., Chen, S., Dong, P., 2010. Temporal variation of sediment load in the Yellow River
1016 basin, China, and its impacts on the lower reaches and the river delta. CATENA 83, 135–
1017 147. https://doi.org/10.1016/j.catena.2010.08.006

1018 Phan, D.B., Wu, C.C., Hsieh, S.C., 2010. Land Use Change Effects on Discharge and
1019 Sediment Yield of Song Cau Catchment in Northern Vietnam. J. Environ. Sci. Eng. 5, 92–
1020 101.

1021 Podwojewski, P., Orange, D., Jouquet, P., Valentin, C., Nguyen, V.T., Janeau, J.L., Tran, D.T.,
1022 2008. Land-use impacts on surface runoff and soil detachment within agricultural sloping

1023 lands in Northern Vietnam. Catena 74, 109–118.
1024 https://doi.org/10.1016/j.catena.2008.03.013

1025 Ranzi, R., Le, T.H., Rulli, M.C., 2012. A RUSLE approach to model suspended sediment load in
1026 the Lo river (Vietnam): Effects of reservoirs and land use changes. J. Hydrol. 422–423,
1027 17–29. https://doi.org/10.1016/j.jhydrol.2011.12.009

1028 Ren, J., He, D., Fu, K., Li, Y., 2007. Sediment variation in the Yuanjiang (the Red River Basin)
1029 driven by climate change and human activities (in Chinese). Chinese Sci. Bull. 52, 142–
1030 147. https://doi.org/https://doi.org/10.1360/csb2007-52-zkII-142

1031 Ringnér, M., 2008. What is principal component analysis? Nat. Biotechnol. 26, 303–304.
1032 https://doi.org/10.1038/nbt0308-303

1033 Simons, G., Bastiaanssen, W., Ngô, L., Hain, C., Anderson, M., Senay, G., 2016. Integrating
1034 Global Satellite-Derived Data Products as a Pre-Analysis for Hydrological Modelling
1035 Studies: A Case Study for the Red River Basin. Remote Sens. 8, 279.
1036 https://doi.org/10.3390/rs8040279

1037 Syvitski, J.P., Morehead, M.D., Bahr, D.B., Mulder, T., 2000. Estimating fluvial sediment
1038 transport: The rating parameters. Water Resour. Res. 36, 2747–2760.
1039 https://doi.org/10.1029/2000WR900133

1040 Syvitski, J.P.M., Peckham, S.D., Hilberman, R., Mulder, T., 2003. Predicting the terrestrial flux of
1041 sediment to the global ocean: A planetary perspective. Sediment. Geol. 162, 5–24.
1042 https://doi.org/10.1016/S0037-0738(03)00232-X

1043 Syvitski, J.P.M., Vorosmarty, C.J., Kettner, A.J., Green, P., 2005. Impact of Humans on the Flux
1044 of Terrestrial Sediment to the Global Coastal Ocean. Science. 308, 376–380.
1045 https://doi.org/10.1126/science.1109454

1046 the World Commission on Dams, 2000. Dams and Development: A New Framework for
1047 Decision-Making.

1048 Tuan, V.D., Hilger, T., MacDonald, L., Clemens, G., Shiraishi, E., Vien, T.D., Stahr, K., Cadisch,
1049 G., 2014. Mitigation potential of soil conservation in maize cropping on steep slopes. F.
1050 Crop. Res. 156, 91–102. https://doi.org/10.1016/j.fcr.2013.11.002

1051 Valentin, C., Agus, F., Alamban, R., Boosaner, A., Bricquet, J.P., Chaplot, V., de Guzman, T., de
1052 Rouw, A., Janeau, J.L., Orange, D., Phachomphonh, K., Do Duy Phai, Podwojewski, P.,
1053 Ribolzi, O., Silvera, N., Subagyono, K., Thiébaux, J.P., Tran Duc Toan, Vadari, T., 2008.
1054 Runoff and sediment losses from 27 upland catchments in Southeast Asia: Impact of rapid
1055 land use changes and conservation practices. Agric. Ecosyst. Environ. 128, 225–238.
1056 https://doi.org/10.1016/j.agee.2008.06.004

1057 Vigiak, O., Malagó, A., Bouraoui, F., Vanmaercke, M., Poesen, J., 2015. Adapting SWAT
1058 hillslope erosion model to predict sediment concentrations and yields in large Basins. Sci.
1059 Total Environ. https://doi.org/10.1016/j.scitotenv.2015.08.095

1060 Vinh, V.D., Ouillon, S., Thanh, T.D., Chu, L. V., 2014. Impact of the Hoa Binh dam (Vietnam) on
1061 water and sediment budgets in the Red River basin and delta. Hydrol. Earth Syst. Sci. 18,
1062 3987–4005. https://doi.org/10.5194/hess-18-3987-2014

1063 Vörösmarty, C.J., Meybeck, M., Fekete, B., Sharma, K., Green, P., Syvitski, J.P.M., 2003.
1064 Anthropogenic sediment retention: Major global impact from registered river
1065 impoundments. Glob. Planet. Change 39, 169–190.
1066 https://doi.org/10.1016/S0921-8181(03)00023-7

1067 Walling, D.E., Fang, D., 2003. Recent trends in the suspended sediment loads of the world's
1068 rivers. Glob. Planet. Change 39, 111–126.
1069 https://doi.org/10.1016/S0921-8181(03)00020-1

1070 Wang, H., Wu, X., Bi, N., Li, S., Yuan, P., Wang, A., Syvitski, J.P.M., Saito, Y., Yang, Z., Liu, S.,
1071 Nittrouer, J., 2017. Impacts of the dam-orientated water-sediment regulation scheme on
1072 the lower reaches and delta of the Yellow River (Huanghe): A review. Glob. Planet.
1073 Change 157, 93–113. https://doi.org/10.1016/j.gloplacha.2017.08.005

Wei, X., Sauvage, S., Le, T.P.Q., Ouillon, S., Orange, D., Vinh, V.D., Sanchez-Perez, J.-M., 2019. A Modeling Approach to Diagnose the Impacts of Global Changes on Discharge and Suspended Sediment Concentration within the Red River Basin. Water 11, 958. https://doi.org/10.3390/w11050958

Williams, J.R., 1975. Sediment Routing for Agricultural Watersheds. JAWRA J. Am. Water Resour. Assoc. 11, 965–974. https://doi.org/10.1111/j.1752-1688.1975.tb01817.x

Wold, S., Esbensen, K., Geladi, P., 1987. Principal component analysis. Chemom. Intell. Lab. Syst. 2, 37–52. https://doi.org/10.1016/0169-7439(87)80084-9

Xie, S., 2002. The Hydrological Characteristics of the Red River Basin. Hydrol. (in Chinese) 22, 57–63. https://doi.org/10.3969/j.issn.1000-0852.2002.04.017

Xu, Z.X., Pang, J.P., Liu, C.M., Li, J.Y., 2009. Assessment of runoff and sediment yield in the Miyun Reservoir catchment by using SWAT model. Hydrol. Process. 23, 3619–3630. https://doi.org/10.1002/hyp.7475

Yang, D., Kanae, S., Oki, T., Koike, T., Musiake, K., 2003. Global potential soil erosion with reference to land use and climate changes. Hydrol. Process. 17, 2913–2928. https://doi.org/10.1002/hyp.1441

Zarfl, C., Lumsdon, A.E., Berlekamp, J., Tydecks, L., Tockner, K., 2015. A global boom in hydropower dam construction. Aquat. Sci. 77, 161–170. https://doi.org/10.1007/s00027-014-0377-0

Zhang, W., Zhao, Z., Tan, S., Li, Y., Wang, A., 2017. Study on the soil erosion in the Yuanjiang - Honghe boundary river areas (in Chinese). Geol. Surv. China 4, 64–69. https://doi.org/10.19388 /j.zgdzdc.2017. 03.10

Zimmerman, J.B., Mihelcic, J.R., Smith, J., 2008. Global stressors on water quality and quantity, Environmental Science and Technology. https://doi.org/10.1021/es0871457

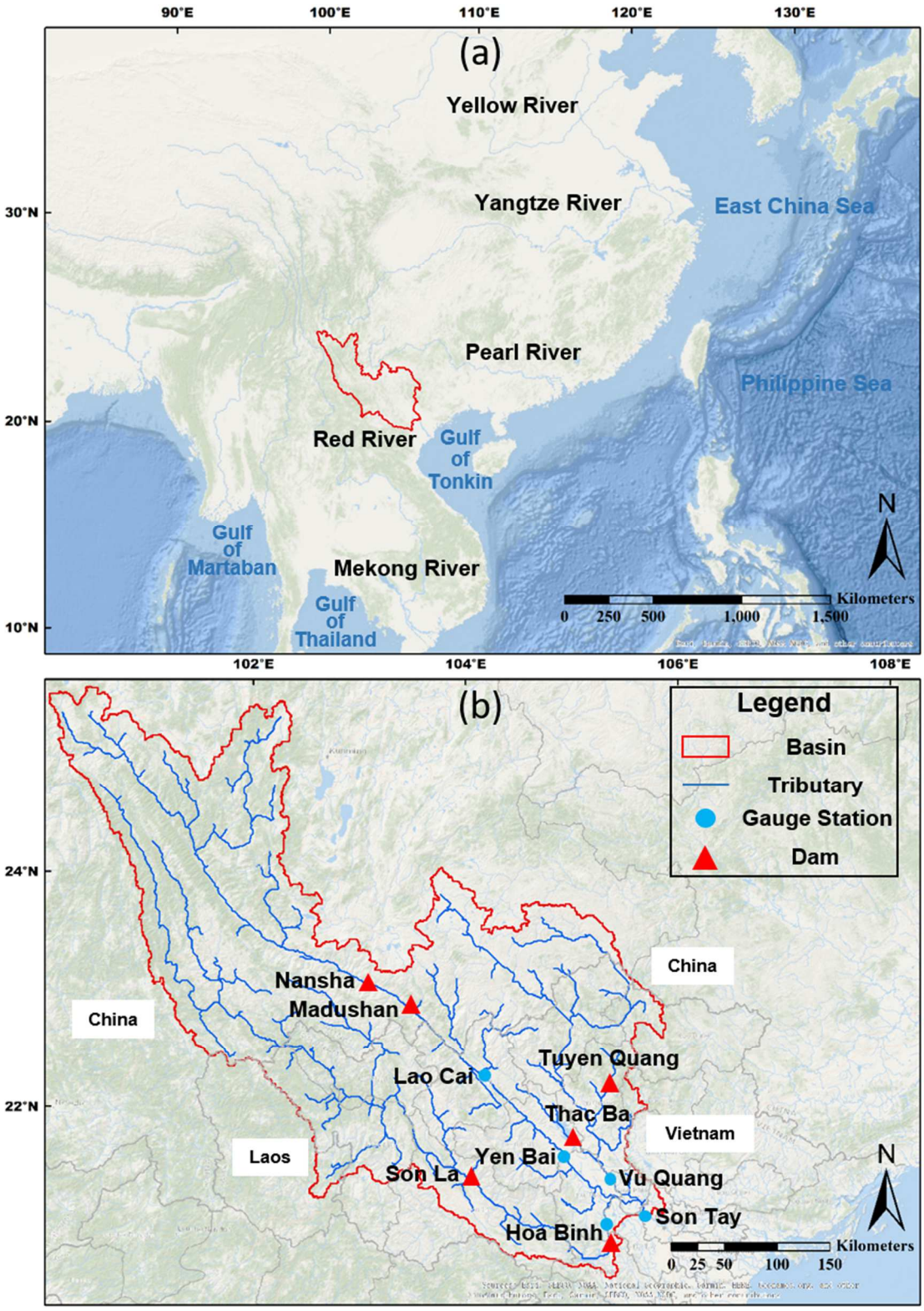

Figure 1. (a) The geographical location of the Red River basin in Southeast Asia; (b) locations of the dams (red triangle) and the hydrological gauge stations (blue point) in the Red River basin. Base maps sources were obtained from ArcGIS desktop.

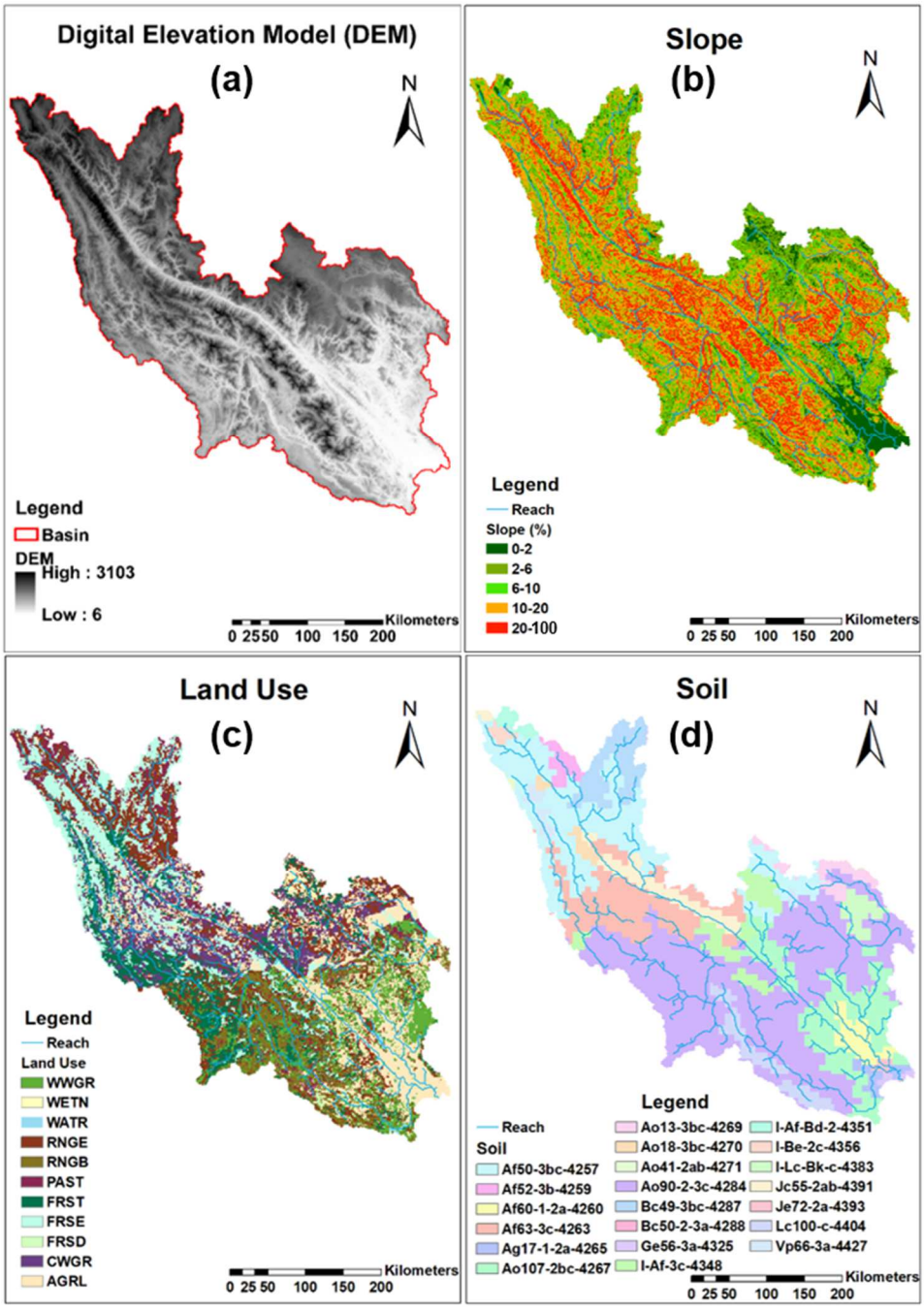

Figure 2: (a) digital elevation model (gray shades); (b) slope classes: slopes were divided into 5 classes by SWAT based on the (DEM); (c) land use map; (d) soil types. Data sources are presented in the supplementary material (Table S-1), and the legends of land use and soil are detailed in the supplementary material (Tables S-2 and S-3).

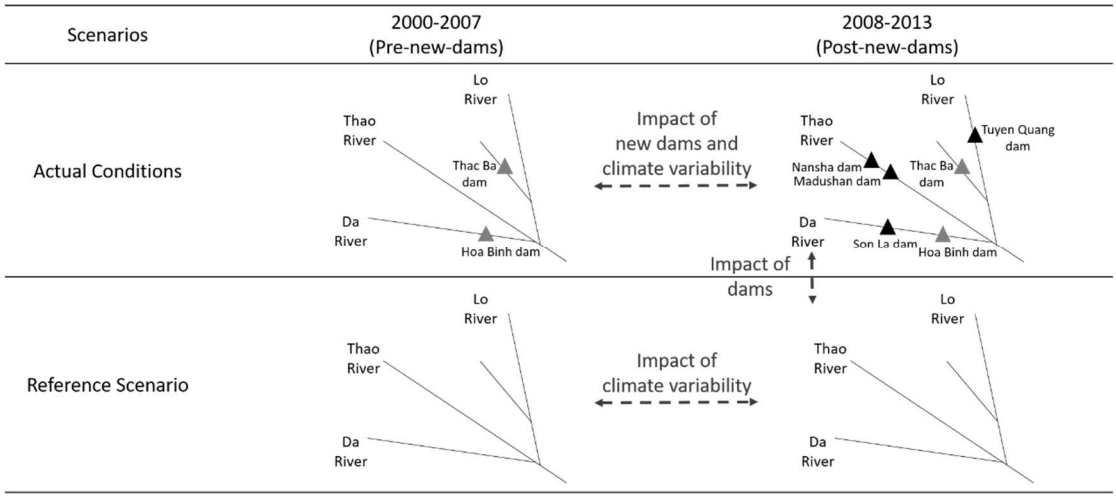

Figure 3. Scenarios setting: actual conditions and reference scenario. Gray triangles are the old dams built before 2000 and black triangles are the new dams built after 2007.

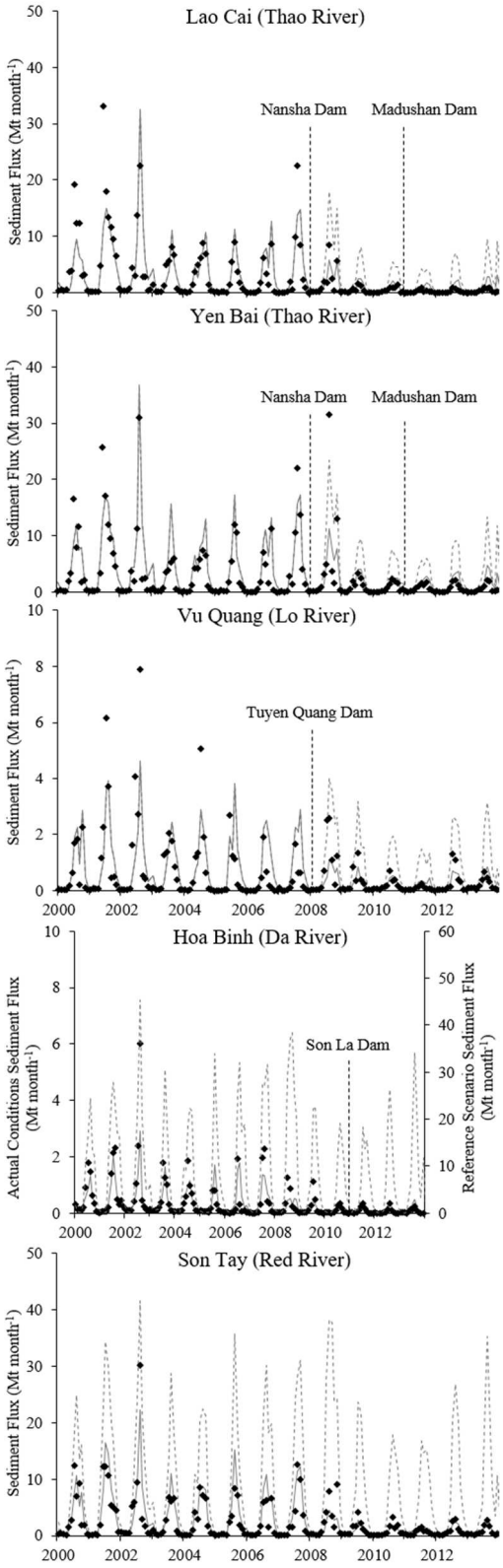

Figure 4. Observed (black dot) and simulated (gray solid line) monthly sediment flux, and simulated sediment flux of reference scenario (without dams, gray dash line) at five stations from 2000 to 2013.

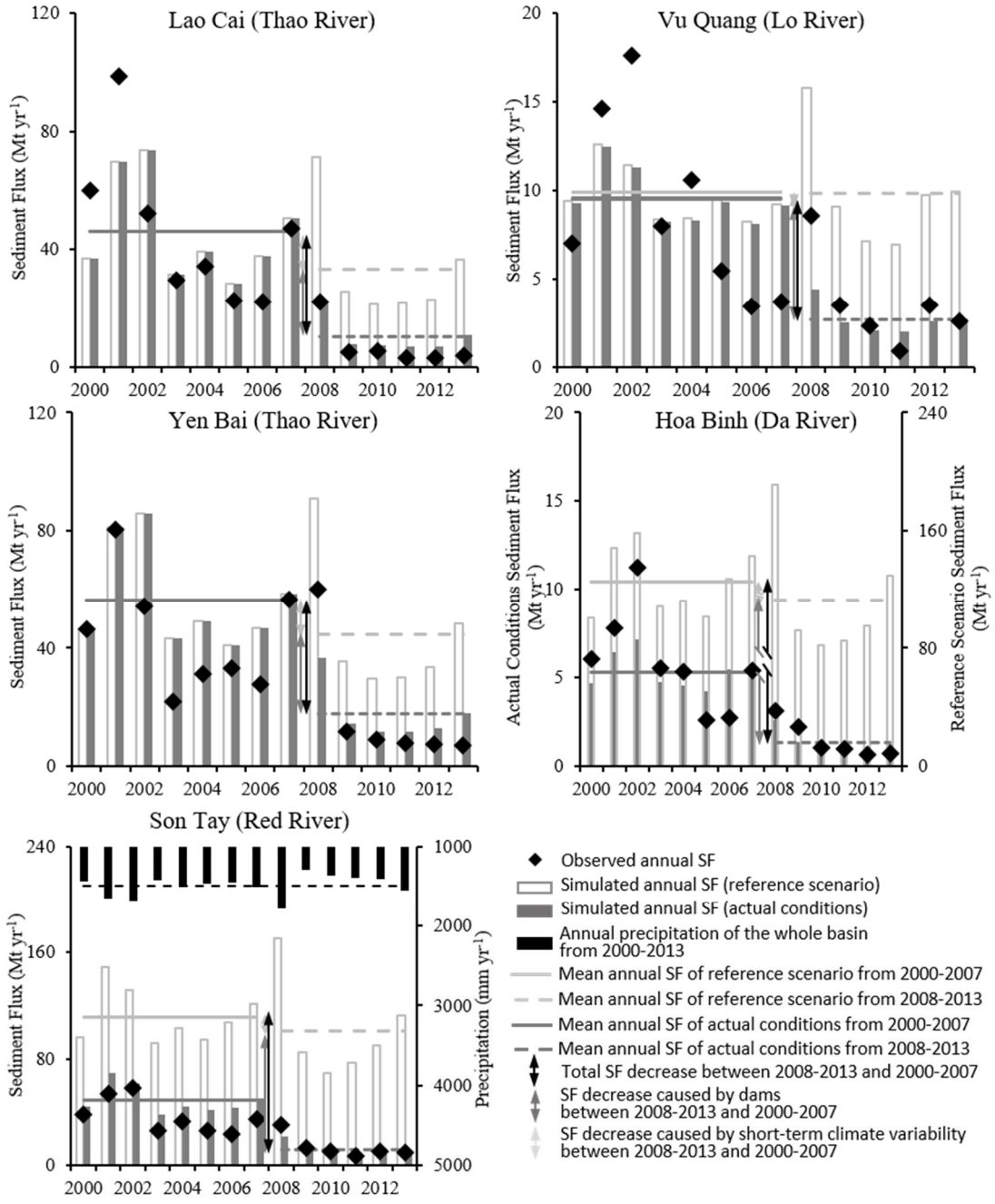

Figure 5. Annual sediment flux (SF) variation from 2000-2013 at 5 gauge stations, and the mean annual SF of pre-new-dams (2000-2007) and post-new-dams (2008-2013). The annual precipitation variation of the whole basin from 2000-2013.

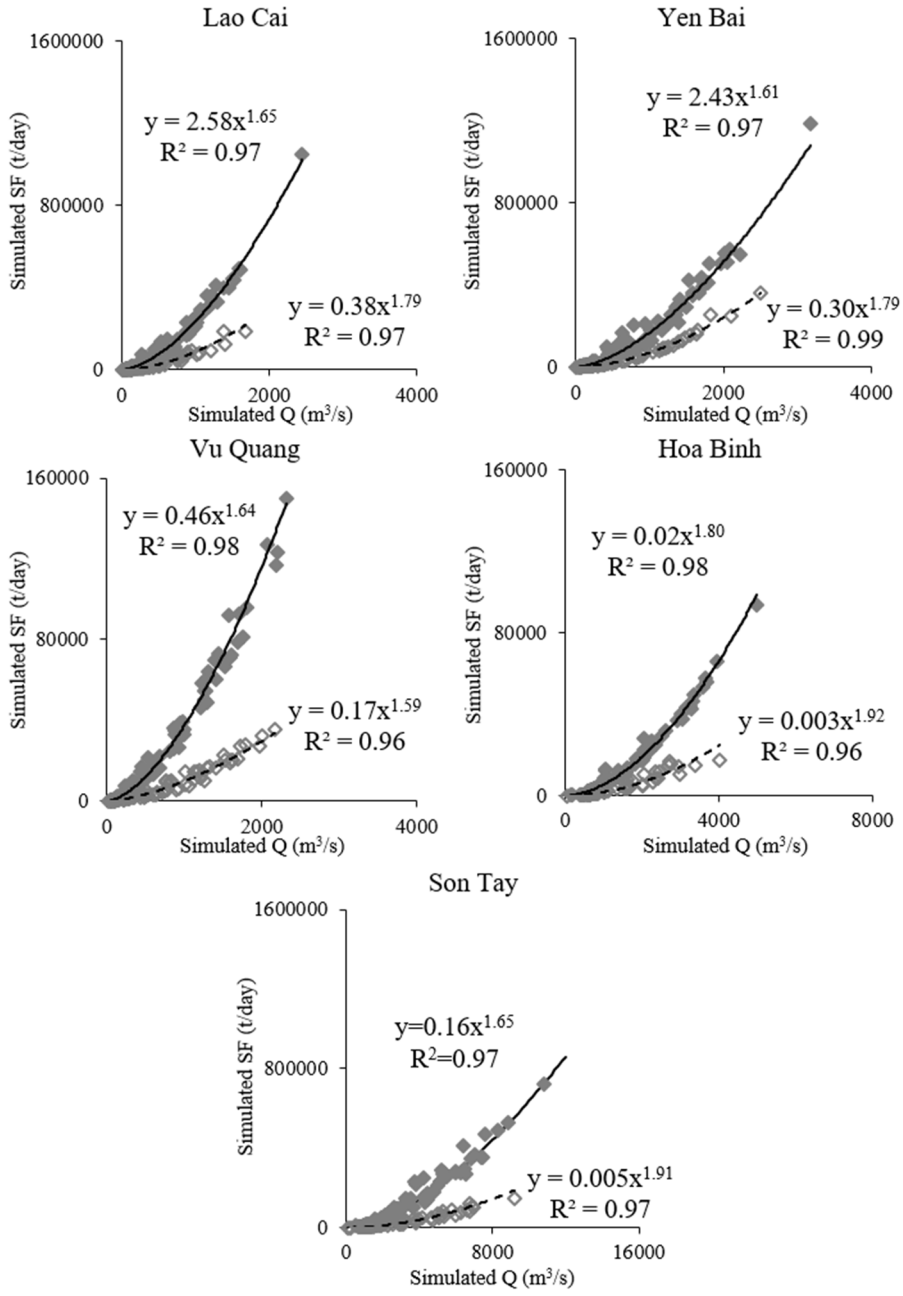

24

25 Figure 6. Correlation and relations between simulated monthly mean discharge (Q) and simulated monthly
26 mean sediment fluxes (SF) at 5 stations in the simulation under actual conditions. Gray solid squares are
27 of the period 2000-2007; gray hollow squares are of the period 2008-2013. Black solid and dash lines are
28 the fitting curves of the period 2000-2007 and 2008-2013, respectively.

29

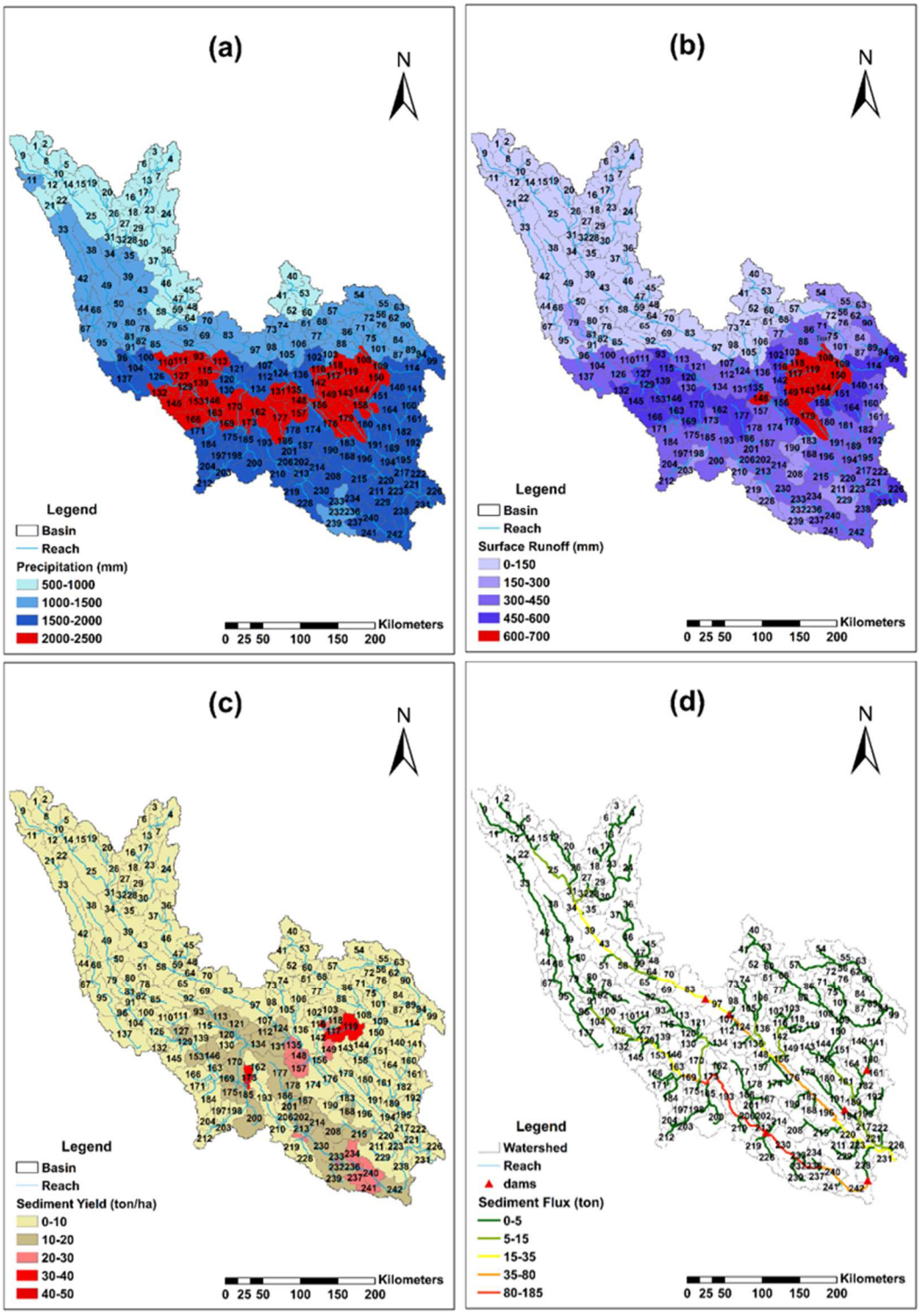

Figure 7. Mean annual value of (a) Precipitation distribution (mm yr^{-1}), (b) Surface Runoff (mm yr^{-1}), (c) Soil Erosion (ton ha^{-1} yr^{-1}), (d) In-stream Sediment Flux (ton yr^{-1}) within 242 sub-basins, derived from the actual conditions simulation over the period 2000-2013.

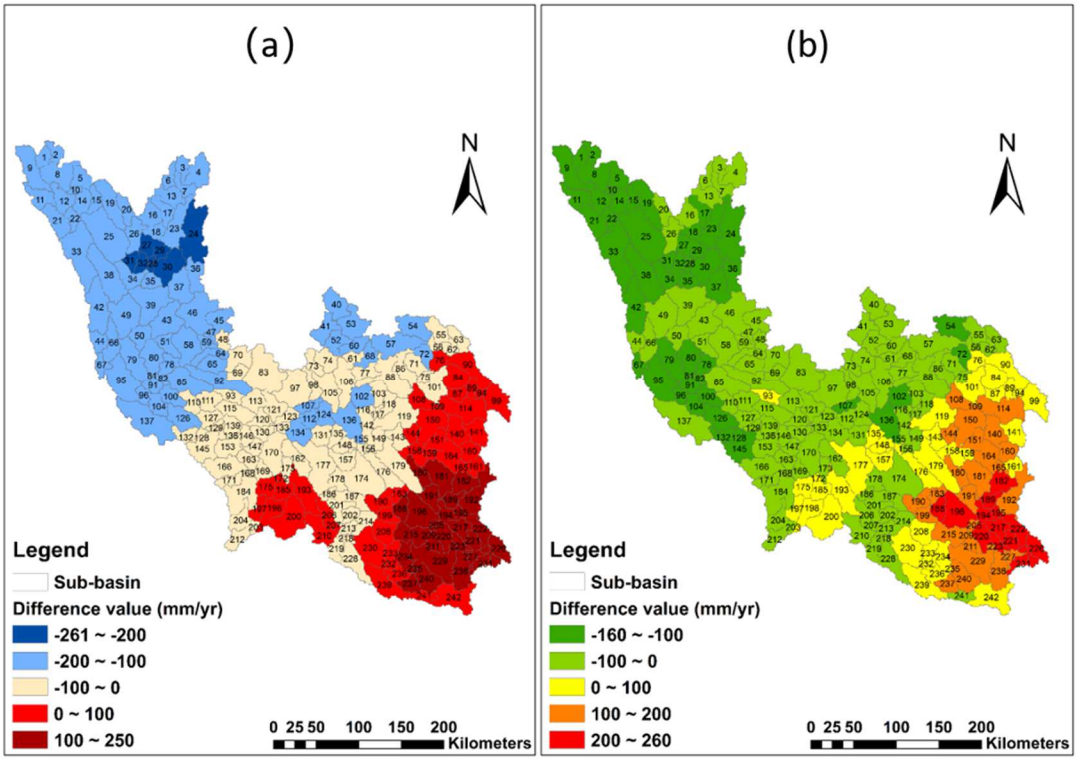

Figure 8. The differences in annual rainfall (a) and annual water availability (b) between 2008-2013 and 2000-2007.

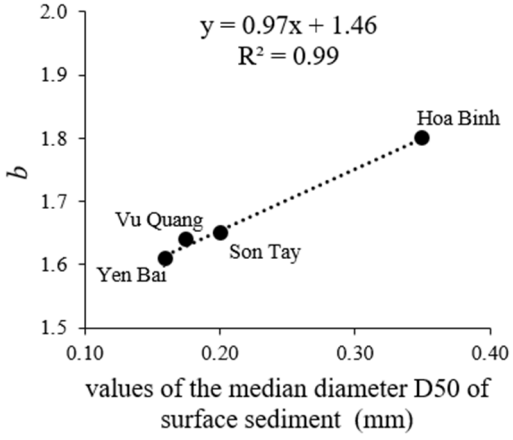

Figure 9. Relationship between the parameter *b* and the values of the median diameter D50 of surface sediment.

Table 1 Basic characteristics of the main dams in the Red River basin (Le et al., 2017; Wei et al., 2019)

Dam	Basin	Construction began	Impoundment	Capacity (km^3)
Nansha	Thao	Feb-06	Nov-07	0.26
Madushan	Thao	Dec-08	Dec-10	0.55
Thac Ba	Lo	1965	1971	2.90
Tuyen Quang	Lo	Dec-02	Mar-08	2.24
Hoa Binh	Da	1980	1989	9.50
Son La	Da	Dec-05	Dec-10	9.26

Table 2 Annual mean and seasonal variation of observed discharge (Q) and suspended sediment concentration (SSC) for 2000-2013 at 5 gauge stations.

Gauge Station (Basin)	Drained Area (km^2)	Q (m^3/s)		SSC (mg/L)	
		Annual Mean	Seasonal Variation	Annual Mean	Seasonal Variation
Lao Cai (Thao)	41600	520	210-1123	800	181-1963
Yen Bai (Thao)	58500	652	218-1577	724	163-1758
Vu Quang (Lo)	30370	891	408-2138	111	22-272
Hoa Binh (Da)	52780	1638	692-3997	42	18-107
Son Tay (Red)	137230	3122	1231-7152	164	55-367

Table 3 Evaluation statistics of sediment flux (SF) on different time scales for each station from 2000 to 2013

Sediment Flux	Statistics	Stations				
		Lao Cai	Yen Bai	Vu Quang	Hoa Binh	Son Tay
Monthly Scale	NSE	0.67	0.66	0.62	0.72	0.71
	R^2	0.68	0.69	0.62	0.75	0.79
	PBIAS	-1.8	-8.7	-0.9	4.6	-24.5
Annual Scale	NSE	0.78	0.60	0.55	0.73	0.54
	R^2	0.78	0.73	0.55	0.77	0.86
	PBIAS	-5.2	-22.6	-0.8	8.6	-24.7

10 Table 4 Seasonal variation of sediment fluxes and mean monthly sediment fluxes for flood and dry
11 seasons at five gauge stations

Gauge Stations	**Drained Area** (km^2)	**Seasonal Variations** ($Mt\ month^{-1}$)	**Flood Season (May-Oct)**		**Dry Season (Nov-Apr)**	
			Flux ($Mt\ month^{-1}$)	Specific Yield ($t\ km^{-2}\ month^{-1}$)	Flux ($Mt\ month^{-1}$)	Specific Yield ($t\ km^{-2}\ month^{-1}$)
Lao Cai	41600	0.0005-34.4	4.5	108.2	0.7	16.8
Yen Bai	48500	0.0007-39.6	5.8	119.6	0.8	16.5
Vu Quang	30370	0.0006-4.7	1.1	36.2	0.1	3.3
Hoa Binh	52780	0.0003-3.0	0.5	9.5	0.1	1.9
Son Tay	137230	0.0014-25.2	4.4	32.1	0.5	3.6

12

Table 5 Simulated sediment flux (Mt yr^{-1}) of reference scenario (without dams) and actual conditions (over the whole study period, 2000-2007 period and 2008-2013 period) compared with other studies and in-situ data; values of trapped sediment (calculated as the difference between average values over 2008-2013 in the reference scenario and actual simulations); impacts of short-term climate variability and dams.

Station (River)	**1960-1972** (Lu et al., 2015)	**1960-1979** (Vinh et al., 2014)	**1960-1970** (Dang et al., 2010)	**2000-2013**			**2000-2007**			**2008-2013**			**Impact**			
				Observed	AC†	RS‡	Observed	AC†	RS‡	Observed	AC†	RS‡	Trapped sediment	Total	Short-term climate variability	Dams
Lao Cai (Thao)	-	-	-	29.2	30.7	40.5	45.7	46.0	46.0	7.1	10.3	33.3	23.0	-78%	-28%	-50%
Yen Bai (Thao)	44.8	43.4	-	32.5	39.8	51.4	43.9	56.5	56.5	17.2	17.6	44.6	27.0	-69%	-21%	-48%
Vu Quang (Lo)	10.1	9.2	-	6.6	6.6	9.7	8.8	9.6	9.5	3.6	2.7	9.8	7.1	-72%	2%	-74%
Hoa Binh (Da)	71.8	65.0	-	4.0	3.6	119.5	5.8	5.3	124.9	1.5	1.3	112.3	111.0	-99%	-10%	-89%
Son Tay (Red)	120.8	119.3	111.6	26.5	33.0	106.9	36.5	49.1	111.6	13.2	11.6	100.6	89.0	-90%	-10%	-80%

AC†: Actual Conditions

RS‡: Reference Scenario (without dams)

20 Table 6 The principal component (PC) loading

Factor	Eigenvectors (percentage of variances %)		
	PC1 (41.6%)	PC2 (25.9%)	PC3 (10.8%)
Soil Erosion (SE)†	0.177	0.399	0.163
Precipitation (P)‡	0.430	0.244	0.101
Water Yield (WY)‡	0.416	0.262	0.095
Surface Runoff (SR)‡	0.446	0.184	-0.033
Slope†	-0.067	0.491	0.125
Clay%†	-0.389	0.117	0.277
Silt%†	0.019	0.243	-0.877
Sand%†	0.346	-0.280	0.256
USLE_P†	-0.246	0.414	0.158
USLE_K†	-0.275	0.340	0.050

21 †: the simulation from the model

22 ‡: the observation and input data

23 Notes: underlined values correspond to the first three highest factor loadings in the PC.

A modelling-based assessment of suspended sediment transport related to new damming in the Red River basin from 2000-2013

Xi Wei[1*], Sabine Sauvage[1**], Sylvain Ouillon[2,3], Thi Phuong Quynh Le[4], Didier Orange[5], Marine Herrmann[2,3], José-Miguel Sanchez-Perez[1]